Published December 16, 2002

On the Mechanism of MgATP-dependent Gating of CFTR Cl^- Channels

Paola Vergani,[1] Angus C. Nairn,[2] and David C. Gadsby[1]

[1]Laboratory of Cardiac/Membrane Physiology and [2]Laboratory of Molecular and Cellular Neuroscience, Rockefeller University, New York, NY 10021

ABSTRACT CFTR, the product of the gene mutated in cystic fibrosis, is an ATPase that functions as a Cl^- channel in which bursts of openings separate relatively long interburst closed times (τib). Channel gating is controlled by phosphorylation and MgATP, but the underlying molecular mechanisms remain controversial. To investigate them, we expressed CFTR channels in *Xenopus* oocytes and examined, in excised patches, how gating kinetics of phosphorylated channels were affected by changes in [MgATP], by alterations in the chemical structure of the activating nucleotide, and by mutations expected to impair nucleotide hydrolysis and/or diminish nucleotide binding affinity. The rate of opening to a burst ($1/\tau$ib) was a saturable function of [MgATP], but apparent affinity was reduced by mutations in either of CFTR's nucleotide binding domains (NBDs): K464A in NBD1, and K1250A or D1370N in NBD2. Burst duration of neither wild-type nor mutant channels was much influenced by [MgATP]. Poorly hydrolyzable nucleotide analogs, MgAMPPNP, MgAMPPCP, and MgATPγS, could open CFTR channels, but only to a maximal rate of opening ~20-fold lower than attained by MgATP acting on the same channels. NBD2 catalytic site mutations K1250A, D1370N, and E1371S were found to prolong open bursts. Corresponding NBD1 mutations did not affect timing of burst termination in normal, hydrolytic conditions. However, when hydrolysis at NBD2 was impaired, the NBD1 mutation K464A shortened the prolonged open bursts. In light of recent biochemical and structural data, the results suggest that: nucleotide binding to both NBDs precedes channel opening; at saturating nucleotide concentrations the rate of opening to a burst is influenced by the structure of the phosphate chain of the activating nucleotide; normal, rapid exit from bursts occurs after hydrolysis of the nucleotide at NBD2, without requiring a further nucleotide binding step; if hydrolysis at NBD2 is prevented, exit from bursts occurs through a slower pathway, the rate of which is modulated by the structure of the NBD1 catalytic site and its bound nucleotide. Based on these and other results, we propose a mechanism linking hydrolytic and gating cycles via ATP-driven dimerization of CFTR's NBDs.

KEY WORDS: ABC transporters • single-channels kinetics • ATP binding and hydrolysis • nonhydrolyzable analogs • catalytic site mutations

INTRODUCTION

CFTR, the protein product of the gene mutated in cystic fibrosis patients (Riordan et al., 1989), comprises two homologous halves linked by a regulatory domain, each half including a transmembrane domain and a cytosolic nucleotide binding domain (NBD),* alternatively called ATP binding cassette (ABC) (Fig. 1). CFTR belongs to the superfamily of ABC transport proteins and, like other members, shows intrinsic ATP binding and hydrolytic activity (Li et al., 1996). But, unlike other ABC proteins, CFTR functions as a gated ion channel which, when open, allows Cl^- ions to flow passively down their electrochemical gradient. CFTR is also an unusual ion channel, as it will open only after its regulatory domain has been phosphorylated by PKA (Cheng et al., 1991; Tabcharani et al., 1991; Picciotto et al., 1992), and the phosphorylated channel requires the continuous presence of hydrolyzable nucleoside triphosphates to sustain normal gating. Despite much investigation, the relationship between binding and hydrolysis of nucleotide at CFTR's two NBDs and the conformational changes that open and close the channel pore remains controversial and poorly understood (e.g., Aleksandrov and Riordan, 1998; Gadsby and Nairn, 1999; Sheppard and Welsh, 1999).

One limitation is insufficient information on CFTR structure. All ABC protein NBDs feature two highly conserved motifs called Walker A (GXXXXGKS/T) and Walker B (four hydrophobic residues followed by an aspartate), common to a variety of ATP-binding proteins (Walker et al., 1982), and an intervening "signature" sequence (consensus: LSGGQ) unique to ABC proteins. Accordingly, X-ray crystal structures of several isolated NBDs reveal that they all share the same basic fold (e.g., Fig. 1): an F1-ATPase-core α/β subdomain positions the Walker A and B motifs near the nucleotide phosphates, an antiparallel β subdomain inter-

Address correspondence to David C. Gadsby, Laboratory of Cardiac/Membrane Physiology, The Rockefeller University, 1230 York Avenue, New York, NY 10021. Fax: (212) 327-7589; E-mail: gadsby@mail.rockefeller.edu

*Abbreviations used in this paper: ABC, ATP-binding cassette; AMP-PCP, adenosine 5′-(β,γ-methylene)triphosphate; AMPPNP, adenosine 5′-(β,γ-imido)triphosphate; ATPγS, adenosine 5′-[γ-thio]triphosphate; MRP1, multidrug resistance protein 1; NBD, nucleotide binding domain; SUR1, sulfonylurea receptor 1.

J. Gen. Physiol. © The Rockefeller University Press • 0022-1295/2003/01/17/20 $8.00
Volume 120 January 2003 17–36
http://www.jgp.org/cgi/doi/10.1085/jgp.20028673

Published December 16, 2002

acts with the nucleotide base, and an α-helical subdomain harbors the signature sequence (Armstrong et al., 1998; Hung et al., 1998; Diederichs et al., 2000; Hopfner et al., 2000; Gaudet and Wiley 2001; Karpowich et al., 2001; Yuan et al., 2001). Oxygen atoms of the β- and γ-phosphate groups of the bound nucleotide contact the ε-amino group and/or the main chain nitrogen of the invariant Walker A lysine, and the Walker B aspartate helps coordinate the catalytic Mg^{2+} ion by hydrogen bonding to a water molecule in the Mg^{2+} ion's inner coordination shell (Hopfner et al., 2000; Gaudet and Wiley, 2001; Junop et al., 2001; Karpowich et al., 2001).

In the structures of NBD monomers, the ATP binding site is surprisingly open (Fig. 1), suggesting that, in vivo, the catalytic site is likely to be completed by interaction with another domain. Evidence of physical proximity (Hunke et al., 2000; Loo and Clarke, 2001; Qu and Sharom, 2001) and of functional interactions between NBDs (e.g., Senior and Bhagat, 1998; Ueda et al., 1999; Gao et al., 2000; Hou et al., 2000) suggests that a second NBD monomer completes the catalytic site. This is supported by the finding of NBD homodimers in certain crystals (Hung et al., 1998; Diederichs et al., 2000; Hopfner et al., 2000; Chang and Roth, 2001; Junop et al., 2001; Locher et al., 2002). Moreover, in two of the most complete structures of ABC-like proteins (Hopfner et al., 2000; Locher et al., 2002), the two NBDs were found to interact in a head-to-tail configuration that sandwiches two active sites in the dimer interface, each with Walker A and B motifs of one NBD and the signature sequence of the other NBD contacting the same ATP molecule (compare Jones and George, 1999).

Unlike these homodimeric bacterial proteins, however, CFTR belongs to the ABC-C subfamily of human ABC proteins, within which sequence similarity between NH_2- and COOH-terminal NBDs of each member is lower (e.g., NBD1 vs. NBD2 in CFTR: 27% identity) than between corresponding NBDs of different members (e.g., CFTR NBD1 vs. multidrug resistance protein 1 (MRP1) NBD1: 42% identity; CFTR NBD2 vs. MRP1 NBD2: 40%). This structural divergence between NBD1s and NBD2s in the ABC-C subfamily implies a conserved functional asymmetry, with each NBD likely playing a distinct role. Biochemical evidence indeed suggests that, in CFTR and its close relatives MRP1 and sulfonylurea receptor 1 (SUR1), NBD1 is a site of low turnover from which nucleotide dissociates only slowly, whereas NBD2 is a catalytically more active site (Matsuo et al., 1999, 2000; Szabó et al., 1999; Gao et al., 2000; Aleksandrov et al., 2001, 2002; Basso et al., 2002; Hou et al., 2002).

In CFTR, the different consequences of introducing equivalent mutations in either NBD1 or NBD2 hint at this functional asymmetry. In several other ABC proteins, mutation of the Walker A lysine or Walker B aspartate in either NBD abolishes both ATP hydrolysis

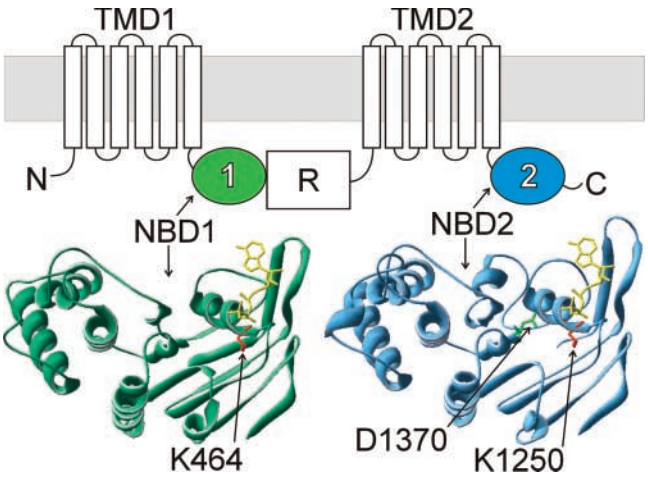

FIGURE 1. (Top) Cartoon of CFTR's domain topology, comprising two transmembrane domains (TMDs), a regulatory (R) domain, and NBD1 (green) and NBD2 (blue). (Below) Ribbon representations of homology models of NBD1 (green) and NBD2 (blue), based on the crystal structure of HisP-ATP (Hung et al., 1998), showing exposed positions of ATP molecules (yellow), Walker A lysines (red), and NBD2 Walker B aspartate (green). Homology models were built using the automated comparative modeling server "Swiss-model" (http://www.expasy.ch/swissmod/SWISS-MODEL.html; Guex and Peitsch, 1997) with alignments optimized on the basis of a ClustalW multiple sequence alignment of 20 bacterial and human NBDs.

and substrate transport (for review see Schneider and Hunke 1998). However, in CFTR the Walker A NBD2 mutation K1250A abolished ATP hydrolysis, whereas the NBD1 mutation K464A simply reduced overall hydrolytic activity (Ramjeesingh et al., 1999); and biochemical studies of Walker B aspartate mutations in CFTR (D572N in NBD1, D1370N in NBD2) have not yet been performed. The consequences of NBD mutations for CFTR channel gating were even more asymmetric. Thus, the K1250A mutation dramatically prolonged burst duration, suggesting that hydrolysis at NBD2 might be coupled to burst termination (Carson et al., 1995; Gunderson and Kopito, 1995), whereas the NBD1 mutations K464A, Q552A, and Q552H somewhat slowed channel opening to a burst, suggesting that NBD1 might be a site of ATP interactions governing opening (Carson et al., 1995; Carson and Welsh 1995). But, since mutations and chemical modifications at NBD2 also strongly affected opening rates, a possible interaction between the two NBDs during channel opening was postulated (Carson et al., 1995; Gunderson and Kopito, 1995; Cotten and Welsh, 1998), and more recent studies of Walker A lysine mutants have suggested that NBD1 might also be involved in controlling burst duration (Powe et al., 2002).

In an attempt to unravel some of this complexity, we have examined the gating kinetics of wild-type (WT) and

Published December 16, 2002

mutant CFTR channels expressed in *Xenopus* oocytes. We studied in detail the dependence of channel gating on [MgATP], gating in the presence of poorly hydrolyzable nucleotide analogs, as well as the effects of mutating residues in the Walker A (K464A and K1250A) and Walker B motifs (in particular, D1370N in NBD2). We addressed two main questions. First, do NBD1 and NBD2 in CFTR regulate separate steps of the channel gating cycle, and are the NBDs independent or do they interact? The second question concerns the relationship between nucleotide binding and hydrolysis and CFTR channel gating. In conventional ligand-gated channels, binding of ligand favors channel opening, and closing is simply the reverse of that process. In CFTR, interaction with ligand (MgATP) is also necessary for gating, but there is disagreement about whether the ligand dissociates unchanged (in which case gating can be described by linear, equilibrium models: Venglarik et al., 1994; Schultz et al., 1995; Aleksandrov and Riordan, 1998) or is hydrolyzed at some point in the gating cycle (cyclical models, violating microscopic reversibility: Baukrowitz et al., 1994; Hwang et al., 1994; Gunderson and Kopito, 1995; Zeltwanger et al., 1999).

We interpret our results to suggest that ATP must bind at both catalytic sites before a CFTR channel can open, that opening is rate limited by a slow step after binding that is sensitive to the structure of the polyphosphate chain, that there is no further nucleotide binding to the open channel, that hydrolysis at NBD2 precedes normal rapid channel closing, and that the integrity of the NBD1 Walker A motif, and nucleotide bound there, influences the rate of exit from locked-open burst states.

MATERIALS AND METHODS

Molecular Biology

Human epithelial CFTR in a *Xenopus* expression vector was used as a template (pGEMHE-WT: Chan et al., 2000) for all point mutations, introduced using a QuickChange site-directed mutagenesis kit (Stratagene). Sequences were checked by automated sequencing. Plasmid DNA was linearized by NheI digestion and in vitro transcribed from the T7 promoter with mMessage mMachine kit (Ambion) as described (Chan et al., 2000).

Xenopus Oocyte Expression

Xenopus laevis oocytes were isolated, collagenase treated, and injected as described (Chan et al., 2000). Amounts of cRNA injected were adjusted to vary the level of expression: up to 40 ng/oocyte was required for high expression of K1250A or K464A/K1250A mutant channels, whereas 0.1–0.25 ng/oocyte sufficed for single channel recordings of WT, K464A, or D1370N channels.

Electrophysiology

Starting 12-h postinjection, recordings in excised inside-out patches were essentially as described (Chan et al., 2000). After removal of the vitelline layer, oocytes were transferred to a petri dish with standard bath solution (designed to minimize cation channel currents) containing (in mM): 138 NMDG, 2 Mg sulfamate, 5 HEPES, 0.5 EGTA, 134 sulfamic acid (pH 7.1 with sulfamic acid). 2–7 MΩ fire-polished pipettes were filled with pipette solution containing (in mM): 138 NMDG, 2 $MgCl_2$, 5 HEPES, 136 HCl (pH 7.4 with HCl). After seal formation (>100 GΩ), patches were excised and transferred to the recording chamber where the cytosolic face was continuously superfused (0.2–0.6 ml/min) with standard bath solution supplemented, when indicated, with PKA catalytic subunit (300 nM) and/or nucleotides, at room temperature (21–26°C). Solutions were switched by computer-driven electric valves (General Valve) and solution exchange time was monitored from decay of endogenous Ca^{2+}-activated Cl^- currents after brief exposure to bath solution supplemented with 2 mM Ca sulfamate. Outward CFTR channel currents were recorded at a membrane potential of 40 mV (pipette potential −40 mV) using an Axopatch 200B amplifier (Axon Instruments, Inc.), filtered at 50 Hz (8-pole Bessel, Frequency Devices), digitized at 1 kHz via a Digidata 1200 interface (Axon Instruments, Inc.), and saved to a PC hard disc using Clampex 7 acquisition software (Axon Instruments, Inc.). MgATP (stock solution in H_20; pH 7.0 with NMDG), Li_4 adenosine 5′-(β,γ-imido)triphosphate (AMPPNP), Li_4 adenosine 5′-[γ-thio]triphosphate (ATPγS), and Na_2 adenosine 5′-(β,γ-methylene)triphosphate (AMPPCP) (stock solutions in standard bath solution supplemented with equimolar Mg sulfamate; pH 7.0 with NMDG) were from Sigma. PKA was purified from bovine heart (Kaczmarek et al., 1980).

Data Analysis

Data analysis was essentially as described (Chan et al., 2000; Csanády et al., 2000). CFTR channels typically open from relatively long closures into open "bursts" interrupted by short "flickery" closures. This is reflected in analyses of records from a single channel that clearly identify, within the bandwidth of our measurements, the presence of a single population of open states (average duration ≈ mean interval between flickery closures) but two distinct populations of closed states. [MgATP] or phosphorylation status do not affect the duration of the short-lived, intraburst flickery closures, or the duration of individual openings within bursts, but they do influence the duration (τib) of the long-lived interburst closures, and phosphorylation increases the number of openings occurring within one burst (Table I; Gunderson and Kopito, 1994; Winter et al., 1994). In this paper we analyze and discuss the dependence on [MgATP] and phosphorylation of the duration, τb, of bursts and of their frequency of occurrence, 1/τib, which we usually refer to as the "rate of channel opening to a burst," but we sometimes simply call it channel "opening rate." Changes in burst duration signal changes in the "rate of channel closing from a burst," sometimes called channel "closing rate." Because we find that the burst duration distributions are described by single exponentials under almost all conditions (see Fig. 4, below; though the lifetimes vary between conditions), this confines extraction of relevant steady state kinetic parameters to determination of mean burst and interburst durations.

For kinetic analysis of patches in which individual channel opening and closing events could be discerned (protocols (a) and (b), below), digitized segments of records were baseline subtracted (to remove slow drifts and small, <0.5 pA, changes in the magnitude of the seal current accompanying solution exchange), and idealized using half-amplitude threshold crossing. The resulting events lists were used to generate dwell-time distributions at all conductance levels that were then simultaneously fitted with a maximum likelihood algorithm (Csanády, 2000) to

Published December 16, 2002

TABLE I

Kinetic Parameters of WT and Mutant CFTR Channels

	WT		K464A		D1370N	
	mean ± SEM	*n*	mean ± SEM	*n*	mean ± SEM	*n*
(A) 5 mM MgATP + 300 nM PKA						
τb	644 ± 63	30	620 ± 58	21	3,768 ± 499	21
τib	1,671 ± 172	30	2,760 ± 439	21	3,588 ± 414	21
	1,552 ± 170	19	2,438 ± 483	12	2,849 ± 491	12
τ_F	19.3 ± 2.0	30	20.8 ± 2.1	21	49.9 ± 4.3	21
n_F	0.57 ± 0.06	30	0.50 ± 0.06	21	2.76 ± 0.25	21
r_{CO}	0.75 ± 0.06	30	0.50 ± 0.05	21	0.38 ± 0.05	21
	0.77 ± 0.08	19	0.54 ± 0.08	12	0.47 ± 0.07	12
r_{OC}	1.95 ± 0.15	30	1.92 ± 0.15	21	0.43 ± 0.07	21
(B) 5 mM MgATP						
τb	338 ± 22	18	309 ± 23	8	1,748 ± 215	17
τib	4,506 ± 497	18	6,752 ± 1314	8	9,503 ± 1440	17
	4,454 ± 1382	5	6,928 ± 1666	6	7,584 ± 1967	9
τ_F	23.5 ± 3.2	18	16.1 ± 2.2	8	51.5 ± 6.0	17
n_F	0.42 ± 0.05	18	0.39 ± 0.06	8	1.40 ± 0.13	17
r_{CO}	0.27 ± 0.03	18	0.18 ± 0.03	8	0.16 ± 0.03	17
	0.33 ± 0.09	5	0.18 ± 0.03	6	0.22 ± 0.05	9
r_{OC}	3.28 ± 0.21	18	3.43 ± 0.25	8	0.75 ± 0.09	17
(C) 50 μM MgATP						
τb	355 ± 44	12	323 ± 136	4	1,433 ± 381	4
τ_F	27.3 ± 5.2	12	22.1 ± 4.4	4	46.2 ± 10.8	4
n_F	0.38 ± 0.05	12	0.45 ± 0.11	4	1.91 ± 0.34	4
(D) 5 mM MgAMPPNP						
τb	1,619 ± 232	32	271 ± 52	8		
τ_F	59.5 ± 6.6	32	26.8 ± 7.7	8		
n_F	2.40 ± 0.26	32	0.38 ± 0.10	8		

Kinetic parameters were obtained using a maximum likelihood simultaneous fit to dwell-time histograms at all conductance levels (Csanády, 2000). Rate constants (r_{CO}, r_{OC}, r_{OF}, r_{FO}) were extracted applying the three-state "C-O-C_F" model (see MATERIALS AND METHODS) and derived parameters were calculated as follows: burst duration, $\tau b = (1/r_{OC})*[1 + (r_{OF}/r_{FO})]$; interburst duration, $\tau ib = 1/r_{CO}$; flicker duration, $\tau_F = 1/r_{FO}$; number of flickers per burst, $n_F = r_{OF}/r_{OC}$. Durations are given in ms, rates in s^{-1}. For τib and r_{CO} values, the top rows give "total" estimates and the bottom ones "best" estimates (as defined in MATERIALS AND METHODS). The values given in C (obtained in experiments as in Fig. 2, A–C) show that frequency and duration of flickery closures do not depend on [MgATP]. The significance of the slight prolongation of τ_F for the D1370N mutant and for WT in 5 mM MgAMPPNP is unknown, but the rate r_{OF} remained 1–2 s^{-1} for all conditions and mutants tested.

determine rate constants (r_{AB}: average number of transitions from state A to state B occurring per unit time of dwell time in state A, measured in s^{-1}). Likelihood of the following three-state "C-O-C_F" scheme was optimized to extract the rate constants indicated:

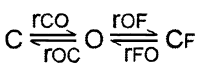

in which "C" is the long interburst closed state, "C_F" is the short flickery closed state, and so the simple r_{CO} and r_{OC} rate constants describe directly the rates of opening to a burst and closing from a burst. However, the parameters derived to describe the observed bursting behavior (burst duration, τb, interburst duration, τib, as well as rates of opening to and closing from a burst) are essentially model independent: only the particular combination of elementary rate constants used to derive them (see Table I, legend), not the numerical values of the parameters, would be different had we instead fitted the alternative three-state "C_1-C_2-O" model to determine burst parameters. An artificial dead time of 6.5 ms (> filter dead time of ~3.6 ms) was imposed to implement a correction for events missed due to the limited bandwidth (Csanády, 2000).

Our measurements can be grouped in three main classes: (a) those from patches containing ≤8 observed channels (Table I, A and B, Fig. 5); (b) those from patches containing >8 observed channels, which we analyzed only in conditions of low open probability (P_o) when opening and closing of individual channels could be discerned and the highest conductance level attained was less than or equal to level 8 (Figs. 2, 7, 8, and 11, Table I, C and D); and (c) records from patches containing hundreds of channels, in which individual gating events could not easily be discerned (Figs. 3, 9, and 10).

(a) Multichannel kinetic analysis from patches containing ≤8 simultaneously open channels. In 5 mM MgATP during PKA application, P_o was relatively high and only patches in which ≤8 simultaneously open channels were observed during the entire recording were analyzed to extract kinetic parameters in this condition (Table I A). For some of these patches, recordings could also be made after washing out the PKA and again after subsequently reapplying it, to examine reversible effects of phosphorylation status on the kinetic parameters (Table I B). In some cases, two estimates are given for τib and its reciprocal r_{CO} that depend strongly on assumptions made about the number of active channels in the patch. One, the "total" estimate, is the mean from all recordings, using the observed maximum number of simultaneously open channels, N′, as an estimate of N, the true number of active channels present. The other, "best" estimate was obtained including only patches in which the presence of an unrecognized channel (hypothesis N > N′) could be excluded with >90% confidence, using statistical tests (Csanády et al., 2000). As excluding records in which the number of channels is not known with confidence tends to select for records in which P_o is highest, the second estimate is a minimum estimate for τib and hence a maximum estimate for r_{CO}.

(b) Multichannel kinetic analysis from patches containing >8 simultaneously open channels. For kinetic analysis in conditions of lower P_o, we used patches with higher numbers of channels to obtain a sufficient number of events. Due to the practical limits imposed by computer processing times (Csanády, 2000), the maximum likelihood fitting programs allow a maximum N of eight. We therefore analyzed records only from patches in which the maximum conductance level did not exceed eight open channels under all test and reference conditions used, and the maximum likelihood fit was done assuming N = 8. We do not report absolute values for τib and r_{CO} in these cases, but only values relative to some other experimental condition applied to the same patch, and these should be relatively insensitive to N. Thus, for MgATP dose-response curves (Fig. 2), rates were normalized to those in bracketing segments at 5 mM MgATP; for the poorly hydrolyzable nucleotides, rates were normalized to those obtained in the same patches at 10 μM (Figs. 7 and 11) or 50 μM MgATP (Fig. 8); for K1250A mutant openings in 10 μM MgATP, rates were normalized to those in nominally MgATP-free bath solution.

(c) Macroscopic current relaxation analysis. To obtain information on τb for mutants or conditions in which slow gating made it difficult to collect a sufficient number of events for the multichannel kinetic analyses described above, we analyzed macroscopic current decay upon nucleotide removal. Records (Figs. 3 and 10), or sums of records (Fig. 9), with several tens of open channels at t = 0 were fitted with single or double exponential decay functions by nonlinear least squares (Sigmaplot; Jandel Scientific).

Published December 16, 2002

Analysis of isolated burst distributions. We also examined the distribution of isolated (i.e., containing no superimposed openings) bursts from experiments of type (a) and (b) (Csanády et al., 2000). For each recording, a threshold duration was chosen to distinguish flickery closures from interburst closures, by minimizing the total number of misclassified events (Jackson et al., 1983). Bursts collected in the same condition from several patches were pooled and fitted, using an unbinned maximum likelihood optimization, with either a single- or a double-exponential distribution. Isolated bursts from records that also included a few superimposed openings were added to the pool only if distribution analysis of that burst population rid of superimposed openings yielded a mean τb within 10% of that obtained by our standard multichannel kinetic analysis. To display the distributions and fits (Fig. 4, A–F), dwell times were ranked from the longest to the shortest and rank number was divided by the total number of bursts included, yielding the ordinate used for the plots, i.e., the fraction of observed bursts with duration greater than or equal to the dwell time given on the abscissa; the plot approximates the survivor function $1 - F(t)$, where $F(t)$ is the distribution function, for the random variable open-burst dwell time (t). Unless otherwise noted, data are given as mean ± SEM (n), where n represents the number of observations.

RESULTS

[MgATP] Dependence of Rate of Opening to a Burst for Catalytic Site Mutants Suggests Involvement of Both NBDs in Channel Opening

WT and mutant CFTR channels in inside-out patches excised from oocytes were activated by phosphorylation to steady state with 300 nM PKA catalytic subunit plus 5 mM MgATP applied to the cytosolic surface. Withdrawal of the kinase, leaving the MgATP, resulted in a rapid partial reduction in channel activity, believed due to incomplete dephosphorylation by persistently active membrane-bound phosphatases (Hwang et al., 1994), after which channel activity remained relatively constant for several minutes (Csanády et al., 2000). After this prephosphorylation, patches were exposed to a range of [MgATP], each test interposed between periods at the reference [MgATP] of 5 mM (Fig. 2 A). CFTR openings occur in bursts, which typically include one or more short shut periods. Reducing [MgATP] did not change the average burst duration, τb (or the duration of the short, intraburst flickery closures, τ_F, or the average duration of individual intraburst openings, see Table I). However, the long closed times separating bursts (interburst duration, τib) were visibly longer at the lower [MgATP] (Fig. 2 A, Table I). Maximum likelihood fitting of dwell-time distributions at all conductance levels (Csanády, 2000) confirmed that the rate of closing from a burst (r_{OC}, in terms of a C-O-C_F scheme, see MATERIALS AND METHODS) was approximately the same at all [MgATP] tested (Fig. 2 E, blue circles), whereas the rate of opening to a burst ($r_{CO} = 1/\tau ib$) was a saturable function of [MgATP] yielding, for WT, an effective dissociation constant ($K_{0.5}$) of 56 ± 5 μM for MgATP (Fig. 2 D, blue circles).

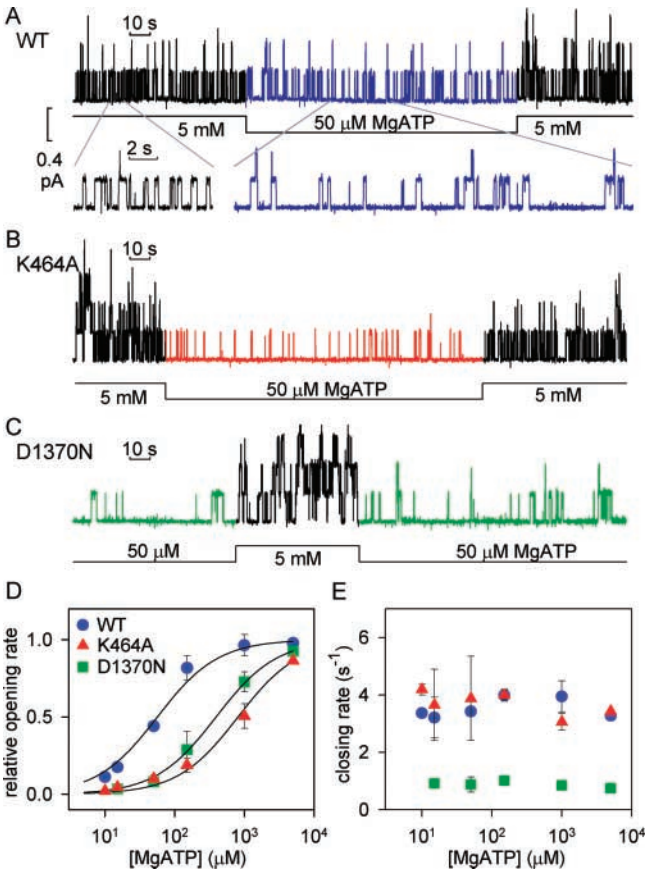

FIGURE 2. [MgATP] dependence of rates of opening to, and closing from, a burst of WT and mutant CFTR channels in inside-out patches. (A) WT channels, prephosphorylated by 300 nM PKA and 5 mM MgATP, shown during exposure to 5 mM, then 50 μM, and again 5 mM MgATP, as indicated; expanded segments at 5 mM and 50 μM MgATP are shown below. (B and C) Representative traces for prephosphorylated K464A and D1370N channels. Relative opening (D) and closing (E) rates (mean ± SEM, $2 \leq n \leq 7$) from analysis of records as in A–C for WT (blue circles), K464A (red triangles), and D1370N (green squares) channels at 10 μM ≤ [MgATP] ≤ 5 mM, plotted on semilogarithmic axes. Opening rate and closing rate at each test [MgATP] were normalized to the mean values measured for bracketing segments at 5 mM MgATP (procedure (b), MATERIALS AND METHODS). Curves in D show Michaelis-Menten fits, yielding $K_{0.5}$ of 56 ± 5, 807 ± 185, 391 ± 118 μM, and r_{COmax} of 1.02, 1.16, and 1.08, for WT, K464A, and D1370N, respectively. For display, the data were further normalized to these r_{COmax} values. Mean absolute opening rates at 5 mM MgATP are given in Table I B. In E, the measured relative closing rates at each [MgATP] have been multiplied by the mean absolute closing rate for each construct in 5 mM MgATP (Table I B).

As the rate of opening, r_{CO}, does not increase linearly with [MgATP], channel opening cannot be a simple bimolecular MgATP-binding reaction, C→O, but must require at least a C1-C2-O scheme (compare Fig. 12 A, below) with distinct MgATP binding (C1→C2) and channel-opening (C2→O) steps. This three-state scheme reduces kinetically to C1→O if MgATP binding is fast

Published December 16, 2002

compared with channel opening, and it predicts a Michaelis-Menten dependence of r_{CO} on [MgATP], as we observe (Fig. 2 D). Evidently, at saturating [MgATP], opening of a WT CFTR channel to a burst is rate limited by a slow MgATP-independent step, but at subsaturating [MgATP] a MgATP binding step appears to limit the rate of channel opening to a burst (Fig. 2 D).

In an attempt to discern at which NBD this binding event occurs, we mutated presumed key catalytic site residues in either NBD. Compared with WT, both K464A (Walker A lysine in NBD1) and D1370N (Walker B aspartate in NBD2) mutant CFTR channels opened less frequently at low [MgATP] (e.g., 50 μM; Figs. 2, A–D), and this defect could be largely overcome by raising the [MgATP], so that, at saturating [MgATP], opening rates of WT, K464A, and D1370N channels differed by less than a factor of two (Table I). Therefore, each of these mutations substantially reduced the apparent affinity for MgATP activation of channel opening (Fig. 2 D), consistent with both mutations altering the binding, rather than the opening, step. As expected (see below) for channels in which opening rate, but not closing rate, is sensitive to [MgATP], the dependence of P_o on [MgATP] was not very different from that of r_{CO}, shown in Fig. 2 D, for WT (see Fig. 3 C), K464A, or D1370N channels.

Similar kinetic analysis of patches containing few channels proved technically difficult for K1250A CFTR (NBD2 Walker A lysine mutant) due to the extremely prolonged bursts (see Fig. 6 C, below), which precluded collection of enough events to reliably estimate absolute values of r_{CO} or P_o. So we recorded macroscopic current in patches with hundreds or thousands of WT or K1250A channels (Fig. 3, A and B), and determined relative P_o as a function of [MgATP] (Fig. 3 C) by normalizing current amplitude at each test [MgATP] to that during bracketing exposures at 5 mM MgATP (Fig. 3, A and B). The curve for K1250A was strongly shifted to higher [MgATP] and was still not saturated at 10 mM MgATP. This shift could reflect effects of the mutation on [MgATP] dependence of rates of opening to and/or closing from bursts. However, single exponential fits to the macroscopic current decay upon nucleotide removal showed that the time constant, which reflects only channel closure from bursts (since, in the absence of MgATP, $r_{CO} = 0$) and provides an estimate of mean burst duration, was unaffected by changes in [MgATP] (Fig. 3 B and legend). Thus, the ratios of the time constants at each [MgATP] between 300 μM and 10 mM to those in the bracketing tests at 5 mM MgATP in the same patches, τ[MgATP]/τ[5mM], averaged 0.9 ± 0.1 ($n = 5$). Therefore, in K1250A, as in WT CFTR, it is only the dependence of channel opening rate on [MgATP] that underlies the [MgATP] dependence of P_o. If indeed r_{CO} is a Michaelis function of [MgATP], and burst duration is [MgATP] independent (Figs. 2 E and 3), the dose-response curve for opening rate would be shifted to higher [MgATP] relative to the curve for P_o: specifically, $K_{0.5rco} \approx K_{0.5Po*}[1 + (r_{COmax}/r_{OC})]$ (Csanády et al., 2000; Dousmanis et al., 2002). In fact, this relationship implies that the effective dissociation constant for MgATP activation of opening of K1250A channels is likely even larger than is apparent in Fig. 3 C because the other effect of the K1250A mutation, marked slowing of channel closure from bursts, would by itself shift the P_o versus [MgATP] curve to lower [MgATP], opposite to our experimental observation.

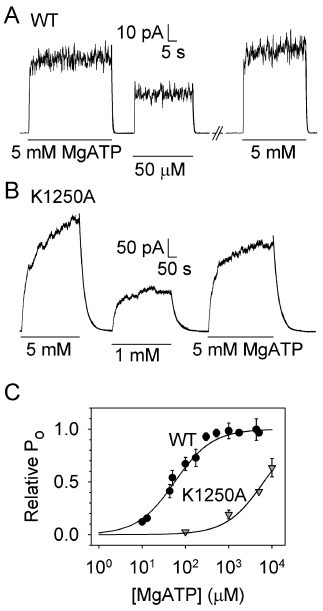

FIGURE 3. The K1250A mutation strongly shifts the [MgATP] dependence of P_o to higher [MgATP]. (A) steady state level of macroscopic current of prephosphorylated WT CFTR channels was ~2-fold lower at 50 μM MgATP than during bracketing exposures to 5 mM MgATP (as expected from Fig. 2); lines below traces mark MgATP applications. Rapid current decay on MgATP washout gave (exponential fit lines superimposed on traces) τ = 0.45 s, τ = 0.40 s, τ = 0.38 s, from left to right (mean τ = 0.54 ± 0.04 s, n = 21, pooled from all [MgATP]). (B) Macroscopic current of K1250A channels was reduced ≥2-fold on lowering [MgATP] from 5 to 1 mM. Superimposed exponential fit lines show slower current decay (note 10-fold contracted time scale relative to A) with, from left to right, τ = 28 s, τ = 30 s, τ = 32 s (mean τ = 39 ± 5, n = 9, from all [MgATP]). (C) Semilog plot of P_o versus [MgATP]. Steady currents (averaged over final ≥20 s) at each [MgATP], normalized to the mean bracketing level at 5 mM MgATP, yielded least-squares. Michaelis fit parameters for WT: $P_{o\,max}$ = 1.04 ± 0.01, $K_{0.5}$ = 57 ± 2 μM; for K1250A: $P_{o\,max}$ = 2.45 ± 0.88, $K_{0.5}$ = 6.5 ± 4.8 mM; for display, WT (circles) and K1250A (inverted triangles) data (mean ± SD, $3 \le n \le 9$) were renormalized to these $P_{o\,max}$ values. Because 10 mM, the highest [MgATP] used, was still far from saturating for K1250A channels, the fit for this mutant is less accurate, evident from large errors on fit parameters.

As increased [MgATP] could largely restore the deficits in opening caused by mutations in either catalytic site, a simple interpretation is that each of the mutations impairs MgATP binding and that both NBD1 and NBD2 catalytic sites must be occupied by MgATP before a CFTR channel can open to a burst.

Influence of [MgATP] and Phosphorylation Status on Burst Duration of WT CFTR Channels

Although the average rate of WT channel closing from bursts does not depend on [MgATP] (Fig. 2 E; see also

Published December 16, 2002

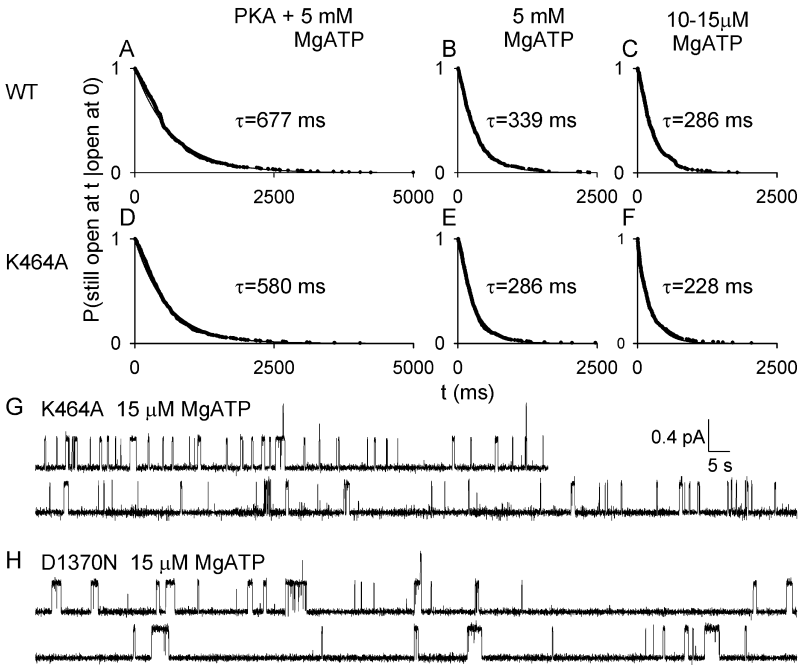

FIGURE 4. Burst duration distributions are similar for WT (A–C) and K464A (D–F) channels under comparable conditions, as indicated (PKA present for left column only). Fitted curves (through data points) show single exponentials from maximum-likelihood fits. Improvement of the fit by inclusion of a second exponential component was judged using the algorithm described in Csanády et al. (2000). Only for K464A at μM MgATP (F) could the likelihood be significantly increased by including a second component, though with a shorter (but not longer; Ikuma and Welsh, 2000) mean: τ_1 = 30 ms, a_1 = 0.17; τ_2 = 263 ms, a_2 = 0.83; increase in log likelihood, ΔLL = 8.3; number of bursts fitted, M = 263; giving (ΔLL − ln(2M) = 2.0). The small differences between means at mM and μM MgATP (B vs. C, E vs. F) may be only apparent, as the mean τb, estimated by multichannel kinetic fits, from these same stretches of record at μM MgATP is not significantly different from that during intervening stretches in 5 mM MgATP (for WT: $\tau b_{\mu M}/\tau b_{5mM}$ = 1.03 ± 0.07, n = 9; for K464A: $\tau b_{\mu M}/\tau b_{5mM}$ = 0.95 ± 0.13, n = 7). (G and H) Representative traces showing gating of K464A and D1370N channels at 15 μM MgATP (after PKA removal). Prolonged bursts of K464A channels (Ikuma and Welsh, 2000) are not evident. Though variability among the four patches containing sufficiently few D1370N channels precluded pooling the data for burst distribution analysis, in none of those patches (analyzed separately) did introduction of a second component significantly improve the maximum likelihood fit.

Anderson and Welsh, 1992; Gunderson and Kopito, 1994; Venglarik et al., 1994; Winter et al., 1994; Csanády et al., 2000; but cf. Zeltwanger et al., 1999), the mean closing rate is reduced roughly twofold by strong phosphorylation (Table I; see also Hwang et al., 1994; Csanády et al., 2000). Because these values are averages extracted from fits to kinetic data from multichannel records, we examined the distribution of isolated burst dwell times to determine whether more than one component was present. Durations of isolated bursts were obtained from records with few, if any, superimposed openings (see MATERIALS AND METHODS and Csanády et al., 2000). Values were pooled for each of three conditions: at saturating, 5 mM, [MgATP] during exposure to PKA (Fig. 4 A) and after PKA washout (Fig. 4 B), and at 10 or 15 μM [MgATP] after PKA washout (Fig. 4 C). In all three conditions, the distribution of WT CFTR channel burst durations revealed a single population, and the distribution means confirmed the results of multichannel kinetic analysis: viz., highly phosphorylated CFTR channels closed on average about twofold more slowly than partially phosphorylated channels (Table I; Fig. 4, A and B), and the average closing rate varied little with [MgATP] (Figs. 2 E, and 4, B and C).

Catalytic Site Mutations at NBD1 Do Not Alter Channel Closing from Normal, MgATP-elicited Bursts

The average rate of closure of K464A mutant CFTR channels from open bursts was closely similar to that of WT CFTR under comparable conditions (Figs. 4, A–F, and 5, A, B, and E); it was likewise approximately independent of [MgATP] (Fig. 2 E, red triangles) and it was similarly reduced roughly twofold by strong phosphorylation (Fig. 4, D and E; Table I). Also like WT, the burst duration distributions of K464A mutant channels were well described by single exponential functions (Fig. 4, D–F).

We performed a limited analysis of the gating kinetics of CFTR channels mutated at two other presumed catalytic site residues in NBD1, the invariant Walker B aspartate, D572 (Fig. 5, C and E), and the adjacent residue, which is a serine (S573, Fig. 5, D and E) in CFTR's NBD1 but is the conserved Walker B glutamate in most NBDs (though it is an aspartate in NBD1 of some ABC-C subfamily members). The mean closing rate from bursts was not substantially altered by these NBD1 mutations (compare Fig. 5 E and Table I): for D572N, r_{OC}(5 mM MgATP + PKA) = 1.4 ± 0.2 s^{-1} (n = 9), and r_{OC}(5 mM MgATP) = 3.1 ± 0.6 s^{-1} (n = 3); for S573E, r_{OC}(5 mM MgATP + PKA) = 2.2 ± 0.3 s^{-1} (n = 7).

Nor was the opening rate of either mutant orders of magnitude lower than that of WT channels in the presence of PKA and saturating [MgATP] (Fig. 5, A–D). Thus, for D572N CFTR, r_{CO}(5 mM MgATP + PKA) = 0.34 ± 0.1 s^{-1} (n = 9), and r_{CO}(5 mM MgATP) = 0.35 ± 0.1 s^{-1} (n = 3), although these values ("total" estimates, see MATERIALS AND METHODS) likely overestimate true opening rate, as the somewhat lower maximal P_o (0.18 vs. 0.29 for WT) of this mutant precluded

Published December 16, 2002

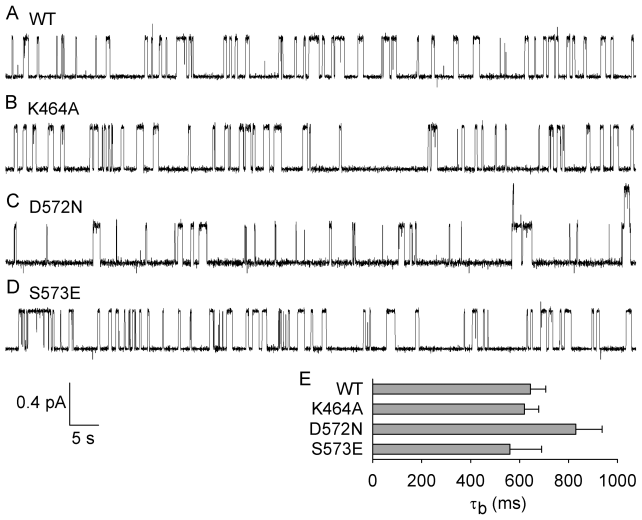

FIGURE 5. Mutations at the NBD1 catalytic site do not markedly alter open burst duration of channels exposed to 5 mM MgATP and 300 nM PKA. Patches contained one WT (A), K464A (B), or S573E (D) channel, or more than one D572N (C) channel. (E) Summary of mean (±SEM) τb values at 5 mM MgATP and 300 nM PKA (n = 30, 21, 9, and 7 for WT, K464A, D572N, and S573E, respectively).

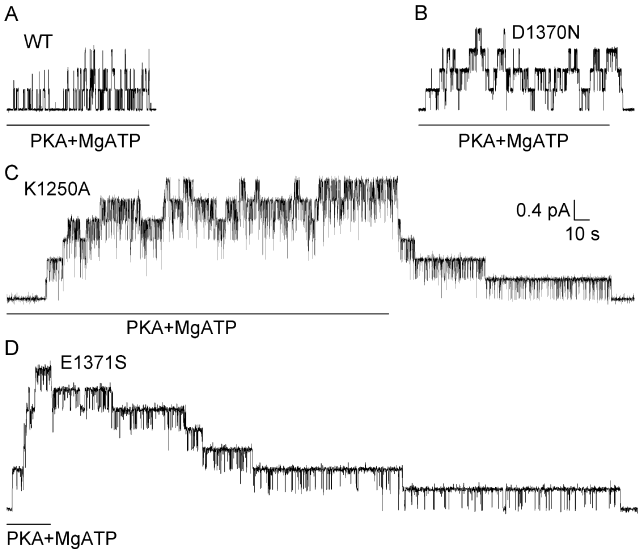

FIGURE 6. Mutations at the NBD2 catalytic site slow channel exit from open bursts. WT (A), D1370N (B), K1250A (C), and E1371S (D) CFTR channels were activated by 5 mM MgATP plus PKA as indicated: burst termination (~0.4-pA downward steps) after nucleotide washout was slowed for NBD2 mutants, relative to WT. Note persistence of brief (intraburst) closures during K1250A and E1371S bursts, long after nucleotide withdrawal.

accurate determination of the number of active channels in each patch. For S573E channels, r_{CO}(5 mM MgATP + PKA) = 0.9 ± 0.2 s^{-1} (n = 7, total estimate) and 1 ± 0.2 s^{-1} (n = 4, best estimate).

Catalytic Site Mutations at NBD2 Slow Channel Closing from Bursts

In contrast to NBD1, corresponding mutations expected to impair hydrolysis in NBD2 substantially slowed exit of CFTR channels from open bursts. D1370N channels closed 4–5-fold more slowly than WT CFTR (Figs. 2 E and 6, A vs. B; Table I), and this reduced closing rate was constant at all [MgATP] tested (Figs. 2 E and 4 H), although, as for WT CFTR, strong phosphorylation slowed closing of D1370N channels roughly twofold (Table I). The K1250A mutation more dramatically slowed channel closing from bursts, resulting in prolonged bursts lasting tens of seconds (Fig. 6 C; cf. Carson et al., 1995; Gunderson and Kopito, 1995; Ramjeesingh et al., 1999; Zeltwanger et al., 1999). Analysis of the macroscopic current relaxation upon nucleotide withdrawal in patches containing many K1250A channels indicates that their average burst duration was ~80 s in the presence of PKA (see below, Fig. 10, E and G) but ~40 s after PKA had been removed (Fig. 3 B), at least two orders of magnitude longer than bursts of WT channels under the same conditions (Fig. 3, A vs. B; Fig. 6, A vs. C). Moreover, for both K1250A and D1370N mutants, this macroscopic current decay followed a single exponential time course, implying the presence of a single population of open bursts (for K1250A, see Figs. 3 B and 10 E; for D1370N, decay time constants were: τ[after 5 mM MgATP + PKA] = 6.4 ± 1.6 s, n = 6; τ[after 5 mM MgATP] = 2.2 ± 0.5 s, n = 7; τ[after 300 μM MgATP] = 1.9 ± 0.3 s, n = 8; cf. Table I). We also found that mutation of the conserved Walker B glutamate in NBD2, E1371, to serine (to mimic the native equivalent residue in NBD1) caused a marked slowing of channel closing from bursts (Fig. 6 D).

Overall, these very different consequences of mutating corresponding key catalytic site residues in NBD1 and NBD2 suggest that, in the gating cycle of a normal WT CFTR channel, termination of the open burst is timed by an event occurring at the NBD2 catalytic site, likely hydrolysis of the nucleotide bound there.

Poorly Hydrolyzable ATP Analogs Can Open WT CFTR Channels, but Only at a Low Rate

Like closing from a burst, opening of a WT CFTR channel to a burst at saturating [MgATP] is also rate limited by a slow step, distinct from nucleotide binding (Fig. 2 D). Similarly, we have shown recently that in cardiac CFTR channels opening to a burst is rate limited by a Mg^{2+}-dependent slow step that is distinct from, and follows, ATP binding (Dousmanis et al., 2002). To further investigate the nature of this slow step, we compared the opening kinetics of WT CFTR channels exposed to MgATP with those of the very same channels exposed to poorly hydrolyzable ATP analogs. In patches containing

Published December 16, 2002

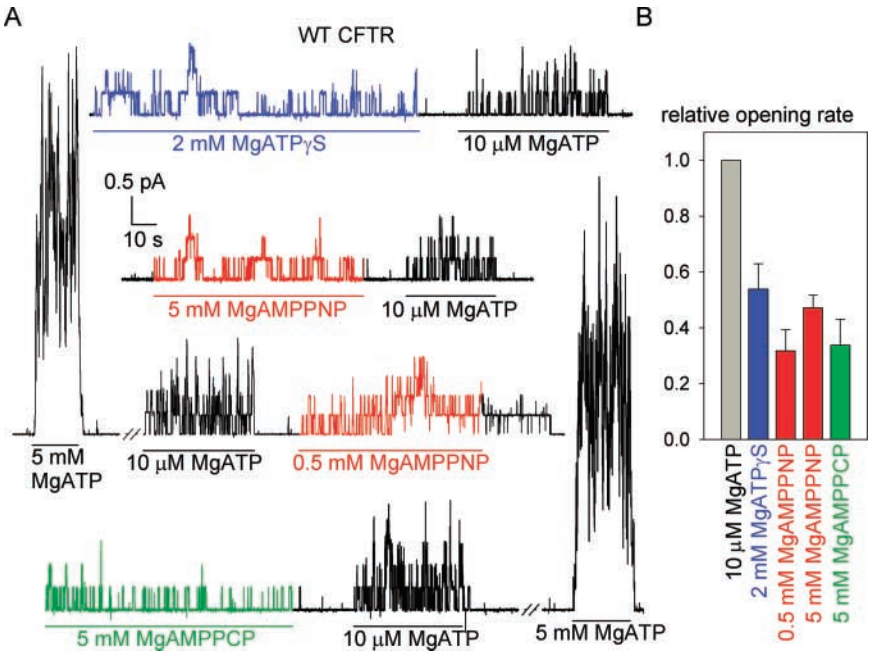

FIGURE 7. Opening of WT CFTR channels by poorly hydrolyzable ATP analogs. (A) Representative recordings from four patches containing many channels, previously phosphorylated by PKA; each patch was exposed to 10 μM MgATP, to (mM) analogue, and to 5 mM MgATP (shown for only two patches). Maximum likelihood fits using C-O-C_F model gave, for MgATPγS $\tau b = 2.0 \pm 0.6$ s ($n = 5$), for MgAMPPNP $\tau b = 1.6 \pm 0.2$ s ($n = 32$), and for MgAMPPCP $\tau b = 0.36 \pm 0.05$ ($n = 11$). (B) Summary of r_{CO} values for nonhydrolyzable analogs normalized to r_{CO} at 10 μM MgATP (which is ~11% of maximum, Fig. 2 D) in the same patch.

hundreds of WT CFTR channels (Fig. 7 A), the superposition of numerous opening and closing transitions at saturating (5 mM) MgATP precluded kinetic analysis, but at 10 μM MgATP individual transitions could be identified and single-channel gating parameters extracted. All channels closed promptly upon ATP removal, and exposure to millimolar concentrations of MgATPγS, MgAMPPNP, or MgAMPPCP elicited measurable channel activity, but in all cases with less frequent bursts than seen at 10 μM MgATP (Fig. 7 A). For each analogue, we measured the rate of opening to a burst relative to that in 10 μM MgATP in the same patch (Fig. 7 B). Using the fact that at 10 μM MgATP r_{CO} is 11.1 ± 3.1% ($n = 3$) of the maximal opening rate attainable at high [MgATP] (Fig. 2 D), we can express the relative opening rate for each analogue as percentage of maximal: 5.3 ± 0.5% ($n = 32$) at 5 mM and 3.5 ± 0.9% ($n = 7$) at 0.5 mM MgAMPPNP, 3.8 ± 1.0% ($n = 11$) at 5 mM MgAMPPCP, and 6.0 ± 1.0% ($n = 5$) at 2 mM MgATPγS.

Two findings argue that this observed low efficacy of millimolar MgAMPPNP in promoting channel opening cannot be overcome by applying even higher concentrations, as might be anticipated if the phosphate chain modification greatly reduced nucleotide binding affinity. First, assuming a hyperbolic relationship between relative opening rate and [MgAMPPNP] (as established for MgATP; Fig. 2 D), the two data points at 0.5 and 5 mM suggest that MgAMPPNP supports a V_{max} of 5.4% of the maximal opening rate in MgATP, with a $K_{0.5}$ = 280 μM. Second, addition of 200 μM MgAMPPNP to a 50 μM MgATP-containing solution (Fig. 8 A) reduced the rate of opening to bursts of WT CFTR channels by ~40% on average (Fig. 8 B). Ignoring the relatively infrequent openings due to the 200 μM MgAMPPNP itself, and treating MgAMPPNP as a simple competitive inhibitor of MgATP action, we estimate an apparent K_i for MgAMPPNP of 230 ± 70 μM ($n = 3$).

The apparent affinity of CFTR channels for MgAMPPCP is comparable. Thus, a mixture of 10 μM MgATP with 5 mM MgAMPPCP was found to be less than half as effective as 10 μM MgATP alone in opening the channels ($r_{CO[5\ mM\ AMPPCP\ +\ 10\mu M\ ATP]}/r_{CO[10\ \mu M\ ATP]} = 0.41 \pm 0.05$, $n = 8$). In this case, with such a high concentration of the analogue, many of the openings would have been due to MgAMPPCP binding alone, i.e., the analogue would have acted both as a ligand causing channels to open and as a competitive inhibitor of ATP-induced opening. From the ratio $r_{CO[5\ mM\ AMPPCP\ +\ 10\ \mu M\ ATP]}/r_{CO[10\ \mu M\ ATP]}$ and the measure of relative opening rate in 5 mM MgAMPPCP alone, we can estimate an effective dissociation constant for MgAMPPCP of ~360 μM.

In principle, the gating we observe in MgAMPPNP alone could reflect contaminating MgATP, as ATP can form during AMPPNP synthesis if conditions are not kept strictly anhydrous (Thomas Billert, personal communication). Indeed Carson and Welsh (1993) reported contamination of AMPPNP by up to 0.5% ATP, and HPLC analysis (JenaBioScience GmbH) of our Sigma-Aldrich AMPPNP preparations revealed a small contamination (≤1%) that might have been ATP. To examine this possibility, AMPPNP stock solutions were pretreated with hexokinase, which transfers the terminal phosphate from ATP, but not from AMPPNP (Yount, 1971), to glucose. Compared with parallel "mock" pretreatments omitting glucose, inclusion of glucose during AMPPNP treatment with hexokinase did not result in a consistent reduction in opening rate ($r_{CO\ HK+}/r_{CO\ HK-} = 0.9 \pm 0.2$, $n = 15$; compared in the

Published December 16, 2002

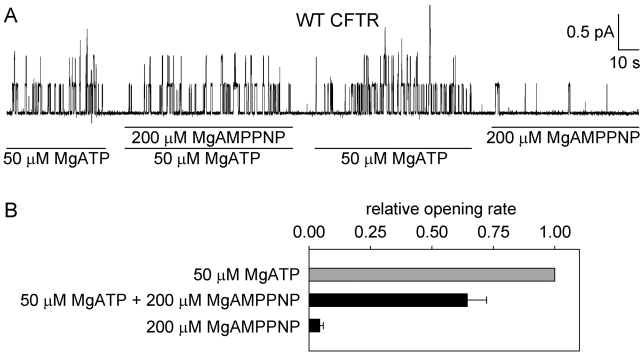

FIGURE 8. MgAMPPNP inhibits MgATP-induced opening of WT channels. (A) Representative record of prephosphorylated channels, exposed alternately to 50 μM MgATP or to 50 μM MgATP plus 200 μM MgAMPPNP, and then to 200 μM MgAMPPNP alone. (B) Summary of r_{CO} values (mean ± SEM, $n = 3$) normalized to the average of that obtained from the stretches in 50 μM MgATP.

same patch). Also, MgAMPPNP from Sigma-Aldrich and MgAMPPNP from Roche Diagnostics were equally effective in stimulating channel opening ($r_{CO\ Sigma}/r_{CO\ Roche} = 1.1 \pm 0.2$, $n = 7$; compared in the same patch), even though HPLC analysis of Roche AMPPNP samples showed no peak at retention times close to that of ATP. These results indicate that the channel openings in MgAMPPNP alone were not due to traces of contaminating ATP but resulted from interaction of CFTR with the imidotriphosphate.

WT Channel Closing from Locked-open Bursts Is Faster After Activation in MgAMPPNP Alone than After Activation in Mixtures of MgAMPPNP with MgATP

During exposure of WT CFTR channels to MgAMPPNP or MgATPγS alone, channel closing from bursts, as well as opening, differs from that seen in MgATP (Fig. 7 A). Thus, during exposures to MgAMPPNP or to MgATPγS (but, interestingly, not to MgAMPPCP) apparently prolonged bursts could be observed. Assuming a single population of open bursts (i.e., a C-O-C_F gating model, possibly an oversimplification) and applying our standard kinetic analysis, we obtained an approximation for the mean burst duration in the presence of each analogue (e.g., Table ID) and normalized it to that at 10 μM MgATP in the same patch, yielding average ratios of 7.5 ± 3.5 ($n = 4$), 4.7 ± 0.6 ($n = 32$), and 1.2 ± 0.2 ($n = 11$) for MgATPγS, MgAMPPNP, and MgAMPPCP, respectively.

In contrast to this 5–10-fold average lengthening of bursts in the presence of MgAMPPNP or MgATPγS alone, mixtures of either analogue with MgATP have been shown to "lock open" WT CFTR channels in prolonged bursts 50–100-fold longer than those in MgATP alone (Gunderson and Kopito, 1994; Hwang et al., 1994; Zeltwanger et al., 1999; Csanády et al., 2000; see also Fig. 10, A and D). To address whether this quantitative difference reflects a direct influence of the simultaneous presence of MgATP and analogue on burst duration, we prephosphorylated WT channels, removed the PKA, and then directly compared closing after exposure to MgATP alone, to MgAMPPNP alone, or to a mixture of MgAMPPNP and MgATP, applied in random order (Fig. 9, inset). For each condition, current traces after nucleotide withdrawal were summed to give ensemble pseudomacroscopic current relaxations (Fig. 9, main panel), which revealed that closing after washout of MgAMPPNP alone (Fig. 9, red trace) was clearly slower than after exposure to MgATP alone (Fig. 9, black trace), in qualitative agreement with the standard kinetic analysis above. However, the relaxation after removal of MgATP + MgAMPPNP (Fig. 9, blue trace), although biexponential, was far slower than expected if the two components reflected closing of two populations of channels, each one independently activated by either just MgATP or just MgAMPPNP. Indeed, the slow component was visibly slower ($\tau_s = 37$ s) than the decay after removal of MgAMPPNP alone ($\tau \sim 7$ s), suggesting that the combined presence of MgATP and MgAMPPNP further stabilized the locked-open channel burst states. This synergy cannot be explained by models in which timing of closing depends on interactions of each channel with a single nucleotide. It implies that interactions between a single channel and at least two nucleotide molecules determine the rate of exit from a locked-open burst.

Closing from Locked-open Bursts Is Faster for K464A Mutants than for WT Channels

Although the K464A mutation did not alter open burst duration of channels exposed to MgATP (Figs. 2 E, 4, and 5), regardless of phosphorylation status (Fig. 4; Table I), it did significantly reduce the duration of certain unusually prolonged bursts. For example, nucleotide withdrawal from patches containing hundreds of WT CFTR channels opened with MgATP plus MgAMPPNP mixture in the presence of PKA resulted in a slow biexponential current decay (Fig. 10 A). On average, 87 ± 4% ($n = 18$) of the total amplitude of the relaxation was attributable to the slow component (Fig. 10 C) whose time constant, $\tau_s = 48.3 \pm 4.5$ s ($n = 18$; Fig. 10 D), provides an estimate of the mean dwell time in the locked-open burst (Csanády et al., 2000). The much smaller fast component (fractional amplitude, $a_f = 0.13$) had a time constant, $\tau_f = 2.0 \pm 0.5$ s ($n = 18$), not greatly different from the normal burst duration of WT channels opened by MgATP in the presence of PKA. For K464A channels, on the other hand (Fig. 10 B), the slow component comprised a somewhat smaller fraction ($a_s = 0.63 \pm 0.04$, n = 16, Fig. 10 C) of the current

Published December 16, 2002

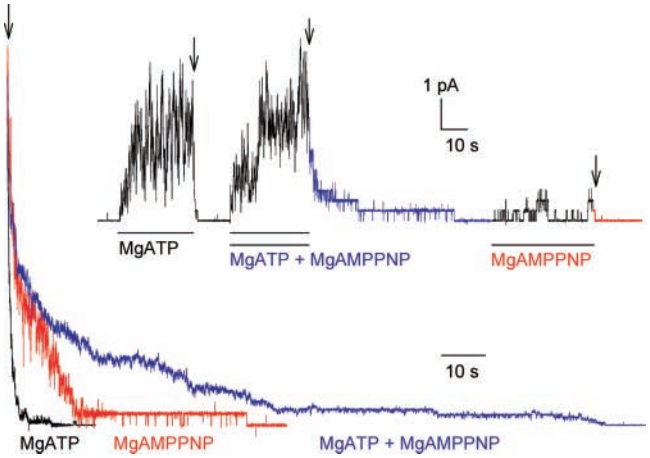

FIGURE 9. Exit from MgAMPPNP-locked burst states is slower when bursts are initiated in the presence of MgATP. Patches with hundreds of prephosphorylated WT CFTR channels were repeatedly subjected to ~30-s long exposures to nucleotides (as in inset), in varied sequence. Each trace in the main figure is the sum of 21 recordings, synchronized upon nucleotide washout (arrow; also in inset), from 12 patches, each exposed to 0.5 mM MgATP, 5 mM MgAMPPNP, or 0.5 mM MgATP + 5 mM MgAMPPNP alternately, an equal number of times. Exponential decay fit parameters are: after MgATP, a = 33 pA, τ = 0.8 s; after AMPPNP, single a = 8 pA, τ = 6.8 s; double a_f = 6 pA, a_s = 6 pA, τ_f = 0.7s, τ_s = 8.8 s; after MgATP + MgAMPPNP, a_f = 20 pA, a_s = 18 pA τ_f = 2 s, τ_s = 36.6 s. As solution exchange time was 0.5–1s, fast components do not accurately reflect channel closing.

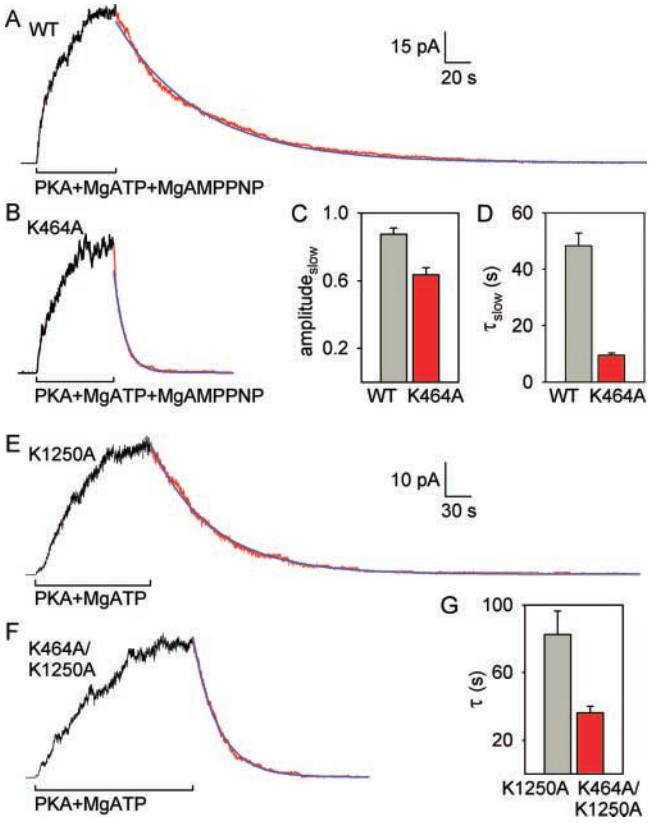

FIGURE 10. The K464A mutation speeds exit from locked open burst states. (A) Macroscopic WT channel current activated by a mixture of 0.5 mM MgATP and 5 mM MgAMPPNP (+PKA) decays slowly upon removal of nucleotides. (B) Current decay is much faster for the K464A mutant in the same conditions. Blue fit lines in A and B show only the slow components of double exponential fits, with τ_s = 67.8s, a_s = 0.92 for WT, and τ_s = 8.7s, a_s = 0.79 for K464A. (C and D) Summaries of fractional amplitude, a_s (C), and time constant, τ_s (D), of the slow component from 18 WT and 16 K464A experiments. In controls with no MgAMPPNP, closure after exposure to MgATP and PKA yielded τ = 1.9 ± 0.2 s (n = 35) for WT and τ = 1.0 ± 0.1 s (n = 34) for K464A, and both constructs sometimes showed a small amplitude slower component: for WT, τ_s = 7.6 ± 1.7 s, a_s = 0.1 ± 0.03 (in 13/35 patches); for K464A, τ_s = 5.9 ± 0.8 s, a_s = 0.24 ± 0.04 (20/24 patches). (E) Macroscopic K1250A currents, activated by 5 mM MgATP + PKA, decay slowly on nucleotide withdrawal. (F) The additional K464A mutation accelerates channel closure from bursts: for the traces shown, τ = 71.7s (K1250A) and τ = 29.7s (K464A/K1250A). (G) Mean time constants of all 9 K1250A and 9 K464A/K1250A relaxations, each well fit by a single exponential.

decay, but its time constant, τ_s = 9.5 ± 0.8 s (n = 16; Fig. 10 D), was markedly reduced.

The smaller fractional amplitude of the slow component for K464A channels can be explained by this observed shortening of their locked-open bursts without the mutation markedly altering the frequency of entry into such bursts. At steady state, the average fraction of time a single channel spends in a particular state is identical to the average fraction of the population of such channels that occupies that state at any instant. Accordingly, because at the moment of nucleotide withdrawal (steady state in the presence of MgATP + MgAMPPNP + PKA) a fraction a_f of open channels was in short bursts (lasting τ_f seconds), and a fraction a_s was in long bursts (lasting τ_s seconds), each single channel may be expected to have spent (at steady state) a_f of its open time in short bursts, and a_s of its open time in long bursts. So the ratio of the fast to slow fractional amplitudes, a_f/a_s, equals the ratio $n\tau_f/m\tau_s$, where n and m are the average numbers of short and long bursts, respectively, entered by each channel in a given (sufficiently long) time interval. We may therefore calculate $m/(n + m)$ = ~0.2 for WT channels, i.e., 1 in every ~5 openings results in a long burst. The analogous estimate for K464A channels gives an average of 1 locking in every ~6 openings. Thus, although mutation of the Walker A lysine at NBD1 substantially shortened locked-open bursts, the mutation apparently altered the frequency of entering these locked bursts little, if at all.

The K464A mutation also shortened (Fig. 10, E–G) the similarly prolonged bursts of NBD2 mutant K1250A channels exposed to MgATP alone (Fig. 6 C). The control record (Fig. 10 E) illustrates the slow decay of macroscopic current after washout of MgATP and PKA from a patch containing hundreds of K1250A CFTR

Published December 16, 2002

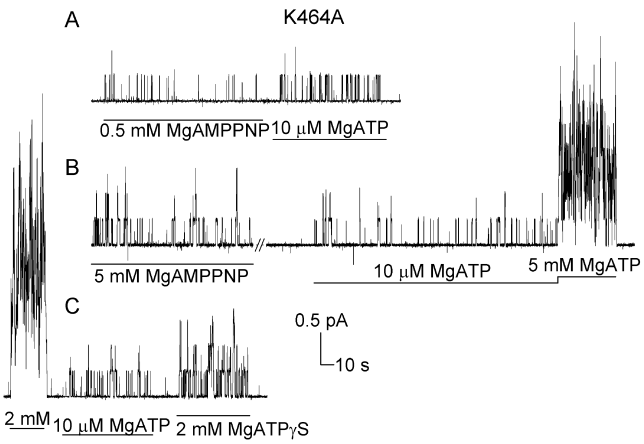

FIGURE 11. Gating of prephosphorylated K464A channels by poorly hydrolyzable ATP analogs, as indicated. Unlike WT (Fig. 7 A), K464A burst duration was not increased during exposure to MgAMPPNP (A and B, $\tau b = 270 \pm 50$ ms, $n = 8$), and was only slightly increased during exposure to ATPγS (C, $\tau b = 655 \pm 170$ ms, $n = 8$), compared with bursts in MgATP ($\tau b = 276 \pm 21$ ms, $n = 16$) in the same patches. Note that, due to the lower apparent affinity of K464A for MgATP (Fig. 2), the relative opening rate of mutant channels at 10 μM MgATP averaged only $2.3 \pm 0.8\%$ ($n = 3$) of that in saturating MgATP (compared with ~11% for WT), so the opening rate of K464A channels was similar in the presence of millimolar concentrations of the poorly hydrolyzable analogs or of 10 μM MgATP.

channels. The current relaxation followed a single exponential time course (Fig. 10 E, blue fit line), with an average time constant $\tau = 83 \pm 14$ s ($n = 9$; Fig. 10 G) (vs. WT $\tau = 1.9 \pm 0.2$ s, $n = 35$). However, in double mutant K464A/K1250A CFTR channels (Fig. 10 F) the current relaxation time constant ($\tau = 36 \pm 4$ s, $n = 9$), and hence the mean open-burst dwell time, was less than half that of channels bearing the K1250A mutation alone (Fig. 10 G).

Closing from Bursts During Activation by Poorly Hydrolyzable Analogs Alone Is Faster for K464A Mutants than for WT Channels

Like WT CFTR (Fig. 7), mutant K464A channels could be opened by millimolar concentrations of the analogs MgAMPPNP or MgATPγS alone (Fig. 11), with rates of opening to bursts of $1.5 \pm 0.2\%$ ($n = 4$) at 0.5 mM and $2.9 \pm 0.3\%$ ($n = 4$) at 5 mM MgAMPPNP, and $5.0 \pm 0.6\%$ ($n = 8$) at 2 mM MgATPγS, of the maximal rate at saturating [MgATP], values not very different from those for WT channels under the same conditions. However, the 5–10-fold prolongation of WT bursts by these analogs (Fig. 7 A) was not evident in K464A channels (Fig. 11): for K464A channels opened by MgAMPPNP or MgATPγS alone, the mean τb values were only 1.1 ± 0.2 ($n = 8$) or 2.2 ± 0.5 ($n = 8$) times larger, respectively, than at 10 μM MgATP. Because this consequence of the K464A mutation is manifest during exposure to essentially nonhydrolyzable ATP analogs it cannot be ascribed to any failure of the mutant channel to hydrolyze nucleotide at the NBD1 catalytic site, but instead must be attributed to the alteration of NBD1 structure per se.

DISCUSSION

We may draw several conclusions from these analyses of gating kinetics of WT and of NBD mutant CFTR channels, in the presence of MgATP and/or of poorly-hydrolyzable analogs: (a) nucleotide binds at both NBD1 and NBD2 catalytic sites before channel opening; (b) the slow opening transition, after nucleotide binding, is highly sensitive to the structures of the β-γ phosphate bridging group and of the γ phosphate; (c) no further nucleotide binding is required to terminate an open burst; (d) hydrolysis of the nucleotide at NBD2 precedes normal, rapid closing from bursts; (e) if that hydrolysis is prevented, the structure of the NBD1 catalytic site and of the nucleotide bound there can modulate rate of exit from the resulting prolonged (locked) open burst. Together, these findings define asymmetric yet interacting roles for the two NBDs in controlling MgATP-dependent channel gating, and they suggest schemes that describe the underlying molecular mechanisms. In the following, we critically evaluate the information and arguments upon which these conclusions are based.

CFTR Cl^- Channel Opening to a Burst

Opening is preceded by nucleotide binding to both catalytic sites. That CFTR channel opening rate varies with [MgATP] (Gunderson and Kopito 1994; Venglarik et al., 1994; Winter et al., 1994; Zeltwanger et al., 1999; Csanády et al., 2000) implies that channel opening to a burst requires at least one MgATP binding step. The saturable dependence of r_{CO} on [MgATP] (Fig. 2 D) means that some (relatively slow) step unrelated to nucleotide binding sets the maximal rate of channel opening at saturating [MgATP]. In principle, that slow step could precede or follow MgATP binding. But, because we find that the maximal rate of opening to bursts is sensitive to the structure of the activating nucleotide (e.g., to details of the polyphosphate chain, see above, or to the presence of an 8-azido moiety: $r_{CO\ max\ Mg8\text{-}azidoATP}/r_{CO\ max\ MgATP} = 0.42 \pm 0.04$, $n = 17$; unpublished observation), this suggests that the rate-limiting opening step follows nucleotide binding. These considerations support our interpretation of CFTR channel opening to a burst as reflecting a relatively slow conformational change after relatively rapid nucleotide binding. In principle, NBD mutations could alter binding or opening steps, or both.

Our results show that mutations within the Walker motifs of either NBD1 (K464A) or NBD2 (D1370N,

Published December 16, 2002

K1250A) reduce the apparent affinity of the MgATP binding site(s) involved in channel opening (Figs. 2 and 3), but (at least for K464A and D1370N) affect the maximal opening rate little (Table I). This combination of effects could be explained if each mutation were to cause a similar energetic destabilization of both the closed channel with MgATP already bound (i.e., reduce MgATP-CFTR binding energy) and the transition state of the subsequent slow opening step (Fersht, 1999). But is it reasonable to expect these mutations to reduce nucleotide-CFTR binding energy? Structural information and nucleotide photolabeling data suggest that it is. Because the Walker A lysine interacts extensively with the β and (when present) γ phosphate groups of the bound nucleotide in all NBD X-ray structures, replacing the large positively-charged side chain with a methyl group may be expected to reduce substrate binding energy by both steric and electrostatic mechanisms (Junop et al., 2001). Accordingly, although no major difference in [α^{32}P]8-azidoATP photolabeling at 0°C was detected between WT and K464A/K1250A (Carson et al., 1995) or K464A CFTR (Vergani et al., 2002), the K464A mutation alone greatly reduced photolabeling of NBD1 by μM [α^{32}P]8-azidoATP at 37°C (Aleksandrov et al., 2002) and virtually abolished stable (i.e., surviving extensive post-incubation washing) photolabeling at 30°C (unpublished data). So, possibly, the lysine does contribute significant nucleotide binding energy but only after a temperature-sensitive conformational change. The Walker B aspartate may also be expected to contribute binding energy for the MgATP complex, since it is thought to help coordinate the catalytic-site Mg^{2+} ion in NBDs, as also observed in F1-ATPase (Weber et al., 1998). Thus, the presence of Mg^{2+} enhanced labeling of NBD2 when CFTR was incubated (at 0° or 37°C) with [α^{32}P]8-azidoATP (Aleksandrov et al., 2002). Plausibly, then, both Walker A lysine and Walker B aspartate do normally contribute to the binding energy of the nucleotide with which they interact.

Therefore, the simplest interpretation of the reduced apparent affinity with which MgATP elicits opening of K464A and D1370N (and K1250A) mutants compared with WT is that the mutations impair nucleotide binding at two different sites, such that at subsaturating [MgATP] channel opening is limited by MgATP binding at NBD1 in K464A, but at NBD2 in D1370N (and K1250A). That nucleotide binding at either NBD can be made rate limiting suggests that in WT CFTR both NBD1 and NBD2 catalytic sites need to be occupied before a channel can open. This provides a straightforward explanation for the similar consequences for channel opening of introducing mutations into the otherwise structurally and functionally divergent NBD1 and NBD2 sequences. Because we also show here that two distinct nucleotides (ATP and AMPPNP) interact with a single WT CFTR channel to determine (locked-open) burst length (Fig. 9), and yet the lack of influence of [MgATP] on burst duration (Figs. 2 E, 3 B, and 4) implies that all nucleotide binding steps occur before the channel opens, these findings lend independent support to our conclusion that a CFTR channel normally opens to a burst only after MgATP has bound to both NBD1 and NBD2 active sites.

Before accepting that conclusion, however, we must consider the possibility that nucleotide occupancy of a single "opening" site suffices to open a WT CFTR channel, and that mutations at the other catalytic site impair opening indirectly by allosterically influencing binding at the opening site. Structural information on NBDs (Armstrong et al., 1998; Hung et al., 1998; Diederichs et al., 2000; Hopfner et al., 2000; Chang and Roth, 2001; Gaudet and Wiley, 2001; Karpowich et al., 2001; Yuan et al., 2001; Locher et al., 2002) argues strongly that K464 and D1370 (and K1250) are, indeed, part of two distinct catalytic sites. Allosteric interactions between CFTR's two NBDs (compare Powe et al., 2002) could, therefore, permit the K464A, D1370N, and K1250A mutations to all affect the same binding site. In CFTR's close ABC-C family relatives, NBD2 reportedly does allosterically influence NBD1 in SUR1 (Ueda et al., 1997, 1999) and MRP1 (Hou et al., 2000); and, in MRP1, there also appears to be a reciprocal allosteric action of NBD1 on NBD2 (Gao et al., 2000; Hou et al., 2002). However, direct measurements of nucleotide occupancy in WT CFTR (assayed by photolabeling with [α^{32}P]8-azidoATP or [α^{32}P]8-azidoADP at 37°C) provide no support for allosteric interactions, as occupancy at NBD1 appeared unaffected by mutation of K1250 in NBD2, and occupancy at NBD2 appeared unaffected by mutation of K464 in NBD1 (Aleksandrov et al., 2002).

Furthermore, several observations argue that nucleotide binding at NBD1 alone is not sufficient for WT CFTR opening, and hence that NBD1 could not be the sole "opening" site. Thus, WT channel opening rate drops to virtually zero within seconds after nucleotide removal (e.g., Fig. 3 A), whereas labeled 8-azidoATP remains bound at the NBD1 catalytic site throughout several minutes of nucleotide-free wash before irradiation (Aleksandrov et al., 2001, 2002; Basso et al., 2002). Moreover, covalent modification of the NBD2 Walker A sequence (Cotten and Welsh, 1998), and the K1250A (Fig. 3 C) and the D1370N (Fig. 2 D) mutations (~8–9 Å apart; e.g., Hung et al., 1998), all reduce apparent affinity for MgATP activation of opening. The simplest explanation is that these three disparate modifications all directly alter the NBD2 ATP binding site rather than that they all allosterically affect the NBD1 site. Most likely, therefore, the rightward shift in [MgATP] dependence of D1370N (and K1250A) open-

Published December 16, 2002

ing rate reflects the lower affinity of a binding step, required for channel opening, at NBD2 itself.

Nor is it likely that, in WT channels, NBD2 could be the sole "opening" site. A major reason is that WT channels with a single ATP molecule bound at the NBD2 catalytic site must be rare, given the higher nucleotide affinity at NBD1 than at NBD2 (Aleksandrov et al., 2001, 2002; Basso et al., 2002). Indeed, because in WT CFTR NBD1 appears to remain nucleotide-bound throughout many gating cycles (Basso et al., 2002), the nucleotide-binding step that controls the timing of WT channel opening at subsaturating [MgATP] most likely occurs at NBD2 (compare Gunderson and Kopito 1995). However, we cannot rule out that, at low [MgATP], mutant K464A CFTR channels might open to bursts with only NBD2 occupied by nucleotide. In fact, although opening rates for WT and D1370N mutant CFTR channels (Fig. 2 D, blue and green symbols) are satisfactorily described by the Michaelis equation (i.e., opening limited by binding to a single site) the opening rates of K464A channels (Fig. 2 D, red symbols) at low (≤50 μM) [MgATP] are slightly higher than expected. If confirmed, these results would be consistent with the right-shifted K464A [MgATP]-r_{CO} curve reflecting principally a reduced nucleotide affinity at NBD1 (now lower than the affinity at NBD2) and a low, but nonzero, opening rate of K464A mutant CFTR channels with nucleotide bound only at the unmodified NBD2 site.

Therefore, present evidence suggests that nucleotide normally binds to both of WT CFTR's NBDs before the channel opens, and that opening is limited by nucleotide binding at NBD2 in WT, D1370N, and K1250A CFTR channels, but probably by nucleotide binding at NBD1 in K464A CFTR channels.

Does CFTR channel opening require ATP hydrolysis? What is the nature of the slow step that rate limits opening of CFTR channels to bursts at saturating [MgATP]? We and others initially proposed that opening is coupled to nucleotide hydrolysis because, at submillimolar concentrations, MgAMPPNP and MgATPγS seemed unable to open CFTR channels that could be opened readily by MgATP and other hydrolyzable nucleoside triphosphates (Anderson et al., 1991; Carson and Welsh, 1993; Gunderson and Kopito, 1994; Hwang et al., 1994). However, millimolar concentrations of the poorly hydrolyzable analogs AMPPNP and ATPγS were recently shown to support CFTR channel opening (Aleksandrov et al., 2000), and we confirm that finding here (Figs. 7–9). But, by directly comparing gating of the same channels, in the same patch, during exposure to MgAMPPNP, MgAMPPCP, or MgATPγS, and to MgATP, we find that at concentrations of these analogs expected to be saturating (Figs. 7 and 8; see also Weinreich et al., 1999; Aleksandrov et al., 2001, 2002) the opening rates of WT (Figs. 7–9) and K464A (Fig. 11) channels are only ∼5% of that reached at saturating [MgATP]. The low frequency of bursts elicited by MgAMPPNP or MgATPγS probably accounts for earlier failures to observe opening in patches with few (≤3) channels during brief exposures to these analogs (Gunderson and Kopito, 1994; Hwang et al., 1994). The failure in patches with many channels, studied at ∼35°C (Anderson et al., 1991; Carson and Welsh, 1993), is perhaps attributable to the weakened interactions between CFTR and MgAMPPNP or MgATPγS at that higher temperature (Schultz et al., 1995; Mathews et al., 1998; Aleksandrov et al., 2000; but cf. Quinton and Reddy, 1992; Hwang et al., 1994). Interestingly, ATP-bound CFTR channels in the absence of Mg^{2+} ions, like MgAMPPNP-bound channels, were found to enter open bursts at a similarly low rate, ∼2% of that seen with MgATP-bound channels (Dousmanis et al., 2002). Although it is unlikely that CFTR can hydrolyze MgAMPPNP, MgAMPPCP, and MgATPγS, at up to 5%, or free ATP at up to 2%, of the rate at which it can hydrolyze MgATP, we cannot rule out on the basis of these results alone that hydrolysis is necessary for channel opening.

Results of mutagenesis experiments provide a stronger challenge to the idea that channel opening requires hydrolysis. Whereas the K464A mutation in NBD1 has been reported to reduce ∼20 fold the ATPase activity of purified CFTR (Ramjeesingh et al., 1999), we find that the same mutation diminishes maximal opening rate by only <50%, similar to effects of other NBD1 catalytic site mutations (Figs. 2 and 5). Moreover, recent comparisons of photolabeling with [α^{32}P]8-azidoATP and [γ^{32}P]8-azidoATP suggest that the catalytic activity of NBD1 in CFTR may be very low, even in WT (Aleksandrov et al., 2002; Basso et al., 2002). This might be related to the nonconserved catalytic-site residues, S573 instead of the Walker B glutamate and S605 instead of the "switch" histidine (Hung et al., 1998; Schneider and Hunke, 1998), as well as, given recent head-to-tail NBD dimers with composite catalytic sites (Hopfner et al., 2000; Locher et al., 2002), to the unusual LSHGH signature sequence in NBD2 (Jones and George, 1999). So it seems unlikely that ATP hydrolysis at NBD1 controls opening of WT CFTR channels.

For NBD2, comparisons of hydrolytic and gating rates are more difficult. For example, our measurements of D1370N CFTR gating show a twofold reduction in maximal opening rate (Table I), but no ATPase measurements are available for D1370N CFTR. However, the corresponding mutation abolished hydrolytic activity in several other ABC ATPases (e.g., Koronakis et al., 1995; Urbatsch et al., 1998; Hrycyna et al., 1999), though it only halved ATPase V_{max} in the DNA mismatch repair protein, MutS (Junop et al., 2001). On

Published December 16, 2002

the other hand, ATPase measurements on purified CFTR have shown that the K1250A mutation abolished ATP hydrolysis (Ramjeesingh et al., 1999), whereas opening of K1250A channels was impaired, but not abolished, at normal [MgATP] (Carson et al., 1995; Gunderson and Kopito, 1995; Ramjeesingh et al., 1999; Powe et al., 2002); indeed, the greatly reduced apparent affinity for MgATP we observed (Fig. 3 C) implies that the maximal opening rate of K1250A may be several-fold greater than that measured at 1–2 mM MgATP. Although these mutagenesis results cannot rule out that opening requires hydrolysis at the NBD2 catalytic site, this is rendered less likely by our conclusions that hydrolysis at NBD2 is linked to termination, rather than initiation, of a burst (see below), and that all nucleotide binding occurs before opening (above).

So, how nucleotides bound at the NBDs allow a CFTR channel to exit its long shut state is still only partially answered. We can conclude that the divalent ion and detailed structure of the β and γ phosphate groups in the activating Mg^{2+}–nucleotide complex influence the energy barrier encountered by a nucleotide-bound channel entering an open burst. One possible interpretation, consistent with results presented here and with the high sensitivity of opening rate to temperature (Aleksandrov and Riordan, 1998; Mathews et al., 1998), is that the opening step corresponds to formation of a prehydrolysis complex (Dousmanis et al., 2002), most likely at the NBD2 catalytic site.

CFTR Cl^- Channel Closing from a Burst

Closing from bursts occurs without further MgATP binding. We found no clear dependence of burst duration on [MgATP] (10 μM to 5 mM) in WT CFTR (Figs. 2 E, 3 A, and 4, B and C) or in K464A, D1370N, or K1250A mutant channels (Figs. 2 E, 3 B, and 4, E–H), indicating that all ATP binding events precede channel opening and no further binding to the open channel is needed to complete the gating cycle. Rate of burst termination was similarly essentially independent of [MgATP] in most other studies (Gunderson and Kopito 1994; Venglarik et al., 1994; Winter et al., 1994; Csanády et al., 2000), but a ≤50% prolongation of average burst duration at [MgATP] above 1 mM (Zeltwanger et al., 1999) was interpreted as reflecting entry into a second, more stable bursting mode favored by MgATP binding at a lower affinity site, proposed to be NBD2. This [MgATP] dependence of burst duration was reported to be exaggerated in K1250A mutant channels, in which brief bursts were observed at 10 μM MgATP and only at higher concentrations did the characteristic (e.g., Fig. 6 C, above) prolonged bursts appear (Zeltwanger et al., 1999; Ikuma and Welsh, 2000; Powe et al., 2002). Though we occasionally observed brief bursts in K1250A channels at 10 μM MgATP (not illustrated), these were very rare, with a frequency of occurrence not demonstrably different from that in nominally MgATP-free bath solution ($r_{CO10\ \mu M}/r_{CObath\ soln} = 0.72 \pm 0.12$, $n = 6$). Thus, brief bursts of K1250A channels might reflect infrequent nucleotide-independent events, unrelated to the physiological gating cycle of WT channels, an interpretation consistent with those brief bursts surviving mutation of the Walker A lysine in either, or both, NBDs (Zeltwanger et al., 1999; Ikuma and Welsh, 2000; Powe et al., 2002).

Moreover, our finding that D1370N channels at low (15 μM) [MgATP] both enter and exit bursts more slowly on average than WT channels (Figs. 2, D–E, and 4 H) demonstrates that this single NBD2 mutation impacts every gating cycle, regardless of the fact that D1370N channels have an intact WT NBD1 sequence. This provides further evidence against the existence, at low [MgATP], of gating cycles in which nucleotide interacts exclusively with NBD1 (Hwang et al., 1994; Gadsby and Nairn, 1994, 1999; Zeltwanger et al., 1999).

Closing from bursts is normally preceded by hydrolysis at the NBD2 catalytic site. A pronounced increase of WT CFTR channel burst duration occurs when the poorly hydrolyzable analogue MgAMPPNP (Figs. 8 and 9 A; Gunderson and Kopito, 1994; Hwang et al., 1994; Carson et al., 1995), or the ATPase inhibitor orthovanadate (VO_4) (Baukrowitz et al., 1994; Gunderson and Kopito, 1994), are added to the MgATP used to activate the channels. Both results suggest that interfering with a hydrolytic cycle delays channel closure from bursts. In other ABC ATPases, VO_4 inhibits steady state hydrolytic activity by forming a tightly bound MgADP–VO_4 complex at the active site, mimicking the bipyramidal pentacovalent transition-state intermediate (e.g., Urbatsch et al., 1995; Chen et al., 2001). In CFTR too, a trapped MgADP–VO_4 complex or tightly bound, nonhydrolyzable, MgAMPPNP molecule might be responsible for locking channels in open bursts by preventing normal completion of a hydrolytic cycle. Comparison of the kinetics of photoaffinity labeling and of channel gating after exposure of WT CFTR to VO_4 in the presence of Mg-8-azidoATP suggests that the Mg-8-azidoADP–VO_4 complex responsible for burst prolongation more likely corresponds to the 8-azido nucleotide labeling of NBD2 than of NBD1: current decays much faster (τ_s ~30 s) than [α^{32}P]8-azido-nucleotide dissociates from NBD1 (τ ~15 min) (Basso et al., 2002), whereas photolabeling at NBD2 is more labile and is lost if a wash precedes UV irradiation (Aleksandrov et al., 2001, 2002). Similarly, presumed disruption of ATP hydrolysis by targeted mutation of key active site residues also slowed exit from bursts, but only if the mutations were at the NBD2 catalytic site (Fig. 5 vs. Fig. 6). Together, these observations strongly suggest that in a locked-open WT channel the nonhydrolyzable ana-

Published December 16, 2002

logue or ADP–VO_4 complex that delays burst termination is tightly bound at the NBD2 site, implying that normal, rapid closure from a burst is preceded by hydrolysis of the nucleotide bound at NBD2 (Carson et al., 1995; Gunderson and Kopito, 1995).

This interpretation has been challenged on three grounds: (a) that AMPPNP binds more tightly to NBD1 than to NBD2 (Aleksandrov et al., 2001, 2002), (b) that CFTR channel closing is only weakly temperature dependent (Aleksandrov and Riordan, 1998), and (c) that CFTR channel gating is an equilibrium process (Aleksandrov and Riordan, 1998).

(a) High affinity interaction of 8-azidoAMPPNP (or AMPPNP) with NBD1 in WT CFTR (Aleksandrov et al., 2001, 2002) does not rule out an action of the analogue at NBD2 in locked-open channels. In fact, such photolabeling data, obtained at 37°C (at which temperature effects of AMPPNP on channel gating are diminished: Schultz et al., 1995; Mathews et al., 1998) on unphosphorylated, and hence mostly closed (Linsdell and Hanrahan, 1998) CFTR channels, are probably unable to detect the small fraction of CFTR molecules occupying locked-open burst states under those conditions. (b) The rate of CFTR channel closing from bursts is strongly temperature dependent (Mathews et al., 1998; Csanády et al., 2000), as expected if this transition is rate limited by hydrolysis. The analysis that suggested weak temperature dependence (Aleksandrov and Riordan, 1998) did not distinguish between the duration of bursts, bounded by relatively long interburst closed times, and the duration of intraburst openings, bounded by brief flickery closures which are probably unrelated to channel interactions with ATP (Table I) as also indicated by their persistence in locked-open channels long after washout of all nucleotides (e.g., Figs. 6, C and D, and 9; Zeltwanger et al., 1999; Dousmanis et al., 2002). (c) The conclusion that CFTR channels gate near equilibrium was derived from analysis of the temperature dependence of P_o, starting from the assumption that P_o reports equilibrium occupancy of closed and open channel states, as in a conventional ligand-gated channel in which closing is simply the opening reaction in reverse (Del Castillo and Katz, 1957). Gating of WT CFTR channels, however, violates microscopic reversibility, as evident from the temporal asymmetry (Gunderson and Kopito, 1995) of transitions between the closed state and two open burst states (distinguishable by their slightly different conductance levels in filtered records). This indicates that the open-burst and closed-interburst states of CFTR channels are not at thermodynamic equilibrium, and that an external source of free energy drives the transitions preferentially in one direction around a cycle. The likely energy source is a MgATP complex, bound by the closed channel before opening to a burst and released only in the

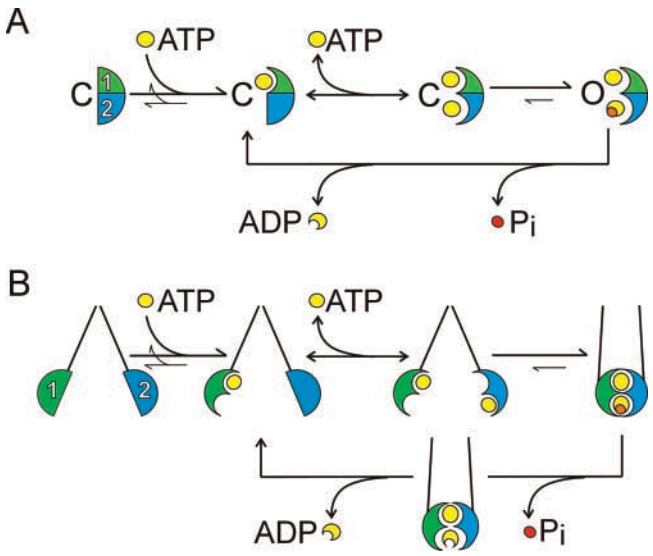

FIGURE 12. (A) Simplified scheme illustrating proposed linking of steps in WT CFTR channel gating, and nucleotide binding and hydrolytic cycles. Yellow ovals depict MgATP complexes, smaller red oval is inorganic phosphate, P_i (colored orange in prehydrolysis complex on open channel); the CFTR protein is represented as a green (NBD1) and blue (NBD2) semicircle, with shape altered (signifying induced-fit conformational changes in the NBDs; Karpowich et al., 2001) upon nucleotide binding. "C" represents closed interburst states of the channel and "O" symbolizes the collection of states during open bursts. Thickness and length of arrows indicate relative rates of individual steps. There is no evidence for strict sequential binding of the two MgATP complexes, but the alternative pathway to the doubly occupied closed state, in which nucleotide binds first at NBD2, probably occurs infrequently in WT CFTR (though not necessarily in mutants) and so was omitted for clarity. (B) Cartoon illustrating a possible physical interpretation of the scheme in A, in which NBD dimerization couples ATP binding and hydrolysis at the catalytic sites to opening and closing of the channel pore. Two semicircles represent NBD1 (green) and NBD2 (blue), and the transmembrane domains are represented by straight-line segments connected to the NBDs. Closed and Open channels are indicated by converging or near-parallel transmembrane domains, respectively. Catalytic sites and Cl^- permeation pathway are structurally connected such that NBD dimer formation results in opening of the channel pore.

form of hydrolysis products as the channel returns to the closed-interburst conformation, so ensuring that the closing reaction is not the reverse of opening.

Unlike other ABC proteins, which hydrolyze ATP to actively transport substrates against their electrochemical potential gradient, CFTR catalyzes dissipative electrodiffusive Cl^- ion movement. Instead, CFTR might harness energy released by ATP hydrolysis to drive conformational changes that would otherwise occur only rarely, making the rate of hydrolysis a timing device, analogous to GTP hydrolysis by G-proteins (Gadsby and Nairn, 1994; Carson and Welsh, 1995; Manavalan et al., 1995). Our results are consistent with a scheme (Fig. 12 A) in which the transition to an open burst, after two MgATP complexes are bound, has a large negative ΔG,

Published December 16, 2002

so that the reverse reaction—exit from the burst with ATP still bound—is very slow. Hydrolysis of the bound triphosphate makes the C→O transition of the channel "reversible," by speeding exit from the otherwise stable open burst states, though via a pathway distinct from that of entry to the burst. In contrast, when hydrolysis is prevented (by the presence at NBD2 of AMPPNP or ADP-VO_4, or of catalytic site mutations), the channel remains locked in the "O" states since exit from the burst can then occur only through very slow reversal (in proper thermodynamic sense) of the transition that initiated the burst.

However, the scheme as drawn suggests tight coupling between channel gating and ATP hydrolysis, which is inconsistent with the largely unaltered gating of the catalytically impaired K464A mutant (with ATPase V_{max} apparently reduced ~20-fold; Ramjeesingh et al., 1999). In fact, evidence suggests that part of the hydrolysis catalyzed by WT CFTR may be uncoupled from channel function. Thus, while phosphorylation of cell-free CFTR by exogenous PKA is an absolute requirement for channel opening (e.g., Linsdell and Hanrahan, 1998), some ATP hydrolysis by partially purified CFTR can be detected also before PKA treatment (Li et al., 1996; Aleksandrov et al., 2002). Levels of phosphorylation above basal might therefore be required to couple events at the NBDs with gating of the transmembrane pore. Even higher levels of steady state phosphorylation could prolong normal hydrolytic bursts (Table I, WT and K464A), as well as nonhydrolytic locked-open bursts (Table I, D1370N; Fig. 10 A vs. Fig. 9; Fig. 3 B vs. Fig. 10 E), by stabilizing the open burst states more than the transition states for both possible pathways (forward or backward; Fig. 12 A) for terminating the burst.

Channel closing from locked-open bursts in nonhydrolytic conditions is modulated by NBD1. Under normal hydrolytic conditions, burst duration was unaffected by mutation of the NBD1 Walker A lysine (Figs. 2, 4, and 5), or of other NBD1 catalytic site residues (Fig. 5), suggesting that the NBD1 catalytic site structure does not, in that case, influence the step that rate-limits burst termination. But when hydrolysis (at NBD2) was prevented, by supplying nucleotide resistant to hydrolysis (Figs. 9, and 10, A–D; Fig. 7 vs. Fig. 11), by adding VO_4 (Vergani et al., 2002), or by mutating the NBD2 Walker A lysine (K1250A; Fig. 10, E–G), the K464A mutation resulted in less prolonged bursts. Very similar reduction of locked-open burst duration by the K464A mutation has been described recently in NIH3T3 and CHO cells (Powe et al., 2002). In addition, the inferred absence of a Mg^{2+} ion from the NBD1–nucleotide complex similarly appeared to shorten the locked-open bursts entered by CFTR channels after Mg^{2+} withdrawal (Dousmanis et al., 2002).

A further indication that the detailed structure of the NBD1–nucleotide complex influences the rate of nonhydrolytic exit from bursts ("unlocking") is that burst duration was prolonged less when MgATP was replaced by just MgAMPPNP than when it was replaced by a mixture of MgATP and MgAMPPNP (Fig. 9); this suggests that slowing of burst termination is greatest when a single CFTR channel interacts simultaneously with an MgATP and an MgAMPPNP complex. The MgAMPPNP complex that prevents hydrolytic burst termination (in both conditions) is unlikely to reside at NBD1, because neither introduction of mutations expected to interfere with hydrolysis at NBD1 (Figs. 2 E, 4, D–F, and 5) nor the presence of a tightly bound nucleotide at NBD1 (~15-min dwell time of labeled 8-azido nucleotide at NBD1; Basso et al., 2002) results in prolonged bursts. We therefore infer that MgAMPPNP bound at NBD2 prevents hydrolysis there (and hence rapid burst termination), while the presence at NBD1 of MgATP, rather than another MgAMPPNP complex, increases dwell time in the locked-open burst.

Although the primary cause of burst prolongation in all these instances appears to be an inhibition of hydrolysis at NBD2, we conclude that the energy barrier for unlocking is influenced by the molecular structure of the NBD1 catalytic site with its bound Mg^{2+}–nucleotide complex. Whether this role of NBD1 is direct, or indirect via allosteric interaction with NBD2, remains to be determined.

Possible Functional Significance of NBD Dimerization

Though the scheme in Fig. 12 A is oversimplified (e.g., it considers neither the short-lived "flickery" closed state, nor the role of phosphorylation by PKA), it nevertheless can account for the data on WT and mutant CFTR channel gating described here. Moreover, we have presented evidence to support each of the components of this simplified scheme, i.e., two nucleotide-binding steps preceding a slow opening step, relatively rapid closing via hydrolysis at NBD2, and much slower nonhydrolytic closing. Unfortunately, the difficulty of collecting adequate numbers of CFTR's relatively infrequent gating events, combined with the lack of biochemical information on CFTR mutants (whether D1370N is capable of ATP hydrolysis, for instance), precludes extraction of the many (≥7) rate constants from fits to data, even for a scheme as simple as the one in Fig. 12 A. However, simulations of that scheme readily reproduce the observed dependence of r_{CO} (Fig. 2 D) or P_o (Fig. 3 C) on [MgATP] for WT CFTR when rate constants are chosen to yield intrinsic dissociation constants of ~10 and 40 μM at NBD1 and NBD2, respectively, maximal opening (~0.3 s^{-1}) and (hydrolytic) closing (~3 s^{-1}) rates as given in Table IB, and a much slower nonhydrolytic closing (reverse of opening) rate

Published December 16, 2002

($\sim$0.003 s^{-1}). The influence of the K464A mutation seen in Fig. 2 D (also on P_o) is then mimicked simply by an $\sim$50-fold acceleration of the MgATP dissociation rate from NBD1, together with the <2-fold observed reduction in maximal opening rate (Table IB). Similarly, the effect of the D1370N mutation seen in Fig. 2 D (and on P_o) can be mimicked by an $\sim$10-fold acceleration of the MgATP dissociation rate from NBD2 with the <2-fold observed reduction in maximal opening rate (Table IB), and (assuming that hydrolysis is abolished) by appropriate speeding of nonhydrolytic closing.

Cyclic formation and dissociation of NBD dimers driven, respectively, by MgATP binding and hydrolysis, was initially proposed as the molecular mechanism coupling catalysis and transport in ABC proteins on the basis of structural and biochemical observations on one of their distant cousins, the DNA double-strand break repair protein Rad50 (Hopfner et al., 2000). Indeed, ATP-driven dimerization was recently demonstrated (Moody et al., 2002) for bacterial ABC transporter NBDs, MJ0796 and MJ1267, in which ATP hydrolysis (but not ATP binding) was prevented by mutation of the Walker B glutamate (analogous to E1371 in CFTR's NBD2, and S573 in NBD1). The mutant NBDs, but not the WT NBDs, formed stable dimers in the presence of ATP, but not of ADP or of the analogs AMPPNP and ATPγS (Moody et al., 2002).

These findings suggest a structural interpretation (cartoon in Fig. 12 B) for the gating scheme presented to account for our experimental results (Fig. 12 A). In this model, binding energy of MgATP in the two catalytic sites drives NBD1-NBD2 dimerization, which in turn is coupled to structural rearrangements, along the lines proposed for other ABC and ABC-like proteins (Hopfner et al., 2000; Locher et al., 2002; Moody et al., 2002), leading to opening of the Cl^- ion permeation pathway in the transmembrane domains and initiation of a burst. The NBD dimer in CFTR would be stabilized by the two MgATP complexes acting as molecular glue (Hopfner et al., 2000; Karpowich et al., 2001). Hydrolysis of the nucleotide bound at NBD2 would then reduce the stability of the dimer, favoring its dissociation coupled to closure of the Cl^- pore in the transmembrane domains and termination of the burst. Prevention of hydrolysis at NBD2 (by mutation of catalytic site residues or by a bound MgAMPPNP or MgADP–VO_4 complex) would be expected to stabilize the NBD dimer, and hence the conformations of the Cl^- channel pore that underlie open-bursts. The low maximal rate of CFTR channel opening to a burst we find with the analogs AMPPNP and ATPγS alone is also consistent with the poor ability of these analogs to form stable dimers of the NBDs MJ0796 and MJ1267 (Moody et al., 2002). Our results also suggest that, in the absence of hydrolysis, the structure of the putative NBD1–NBD2 dimer interface is subtly affected by the residue in the 464 position in NBD1, and by the nucleotide complex bound at NBD1, e.g., whether it is free ATP (Dousmanis et al., 2002), MgATP, or MgAMPPNP, so that the NBD dimer is stabilized—and hence the burst duration prolonged—to differing degrees.

We thank László Csanády and Claudia Basso for much helpful discussion, and Roberto Sánchez and Andrej Sali for help with initial attempts at homology modeling. We also thank David Kopsco and Atsuko Horiuchi for excellent technical assistance.

This work was supported by the National Institutes of Health (DK51767) and the Cystic Fibrosis Association of Greater New York.

Bertil Hille served as guest editor.

Submitted:12 July 2002
Revised: 29 October 2002
Accepted: 30 October 2002

REFERENCES

Aleksandrov, A.A., X. Chang, L. Aleksandrov, and J.R. Riordan. 2000. The non-hydrolytic pathway of cystic fibrosis transmembrane conductance regulator ion channel gating. *J. Physiol.* 528: 259–265.

Aleksandrov, A.A., and J.R. Riordan. 1998. Regulation of CFTR ion channel gating by MgATP. *FEBS Lett.* 431:97–101.

Aleksandrov, L., A.A. Aleksandrov, X.B. Chang, and J.R. Riordan. 2002. The first nucleotide binding domain of cystic fibrosis transmembrane conductance regulator is a site of stable nucleotide interaction, whereas the second is a site of rapid turnover. *J. Biol. Chem.* 277:15419–15425.

Aleksandrov, L., A. Mengos, X.-B. Chang, A. Aleksandrov, and J.R. Riordan. 2001. Differential interactions of nucleotides at the two nucleotide binding domains of the cystic fibrosis transmembrane conductance regulator. *J. Biol. Chem.* 276:12918–12923.

Anderson, M.P., H.A. Berger, D.P. Rich, R.J. Gregory, A.E. Smith, and M.J. Welsh. 1991. Nucleoside triphosphates are required to open the CFTR chloride channel. *Cell.* 67:775–784.

Anderson, M.P., and M.J. Welsh. 1992. Regulation by ATP and ADP of CFTR chloride channels that contain mutant nucleotide-binding domains. *Science.* 257:1701–1704.

Armstrong, S., L. Tabernero, H. Zhang, M. Hermodson, and C. Stauffacher. 1998. Powering the ABC transporters: the 2.5 Å crystal structure of the ABC domain of RBSA. *Pediatr. Pulmonol.* 17: 91–92.

Basso, C., P. Vergani, A.C. Nairn, and D.C. Gadsby. 2002. NBD1 might remain nucleotide-bound throughout CFTR channel gating cycle. *Biophys. J.* 82:12a.

Baukrowitz, T., T.C. Hwang, A.C. Nairn, and D.C. Gadsby. 1994. Coupling of CFTR Cl^- channel gating to an ATP hydrolysis cycle. *Neuron.* 12:473–482.

Carson, M.R., S.M. Travis, and M.J. Welsh. 1995. The two nucleotide-binding domains of cystic fibrosis transmembrane conductance regulator (CFTR) have distinct functions in controlling channel activity. *J. Biol. Chem.* 270:1711–1717.

Carson, M.R., and M.J. Welsh. 1993. 5′-Adenylylimidodiphosphate does not activate CFTR chloride channels in cell-free patches of membrane. *Am. J. Physiol.* 265:L27–L32.

Carson, M.R., and M.J. Welsh. 1995. Structural and functional similarities between the nucleotide-binding domains of CFTR and GTP-binding proteins. *Biophys. J.* 69:2443–2448.

Chan, K.W., L. Csanády, D. Seto-Young, A.C. Nairn, and D.C.

Gadsby. 2000. Severed molecules functionally define the boundaries of the cystic fibrosis transmembrane conductance regulator's NH(2)-terminal nucleotide binding domain. *J. Gen. Physiol.* 116:163–180.

Chang, G., and C.B. Roth. 2001. Structure of MsbA from *E. coli*: a homolog of the multidrug resistance ATP binding cassette (ABC) transporters. *Science.* 293:1793–1800.

Chen, J., S. Sharma, F.A. Quiocho, and A.L. Davidson. 2001. Trapping the transition state of an ATP-binding cassette transporter: evidence for a concerted mechanism of maltose transport. *Proc. Natl. Acad. Sci. USA.* 98:1525–1530.

Cheng, S.H., D.P. Rich, J. Marshall, R.J. Gregory, M.J. Welsh, and A.E. Smith. 1991. Phosphorylation of the R domain by cAMP-dependent protein kinase regulates the CFTR chloride channel. *Cell.* 66:1027–1036.

Cotten, J.F., and M.J. Welsh. 1998. Covalent modification of the nucleotide binding domains of cystic fibrosis transmembrane conductance regulator. *J. Biol. Chem.* 273:31873–31879.

Csanády, L. 2000. Rapid kinetic analysis of multichannel records by a simultaneous fit to all dwell-time histograms. *Biophys. J.* 78:785–799.

Csanády, L., K.W. Chan, D. Seto-Young, D.C. Kopsco, A.C. Nairn, and D.C. Gadsby. 2000. Severed channels probe regulation of gating of cystic fibrosis transmembrane conductance regulator by its cytoplasmic domains. *J. Gen. Physiol.* 116:477–500.

Del Castillo, J., and B. Katz. 1957. Interaction at end-plate receptors between different choline derivatives. *Proceedings of the Royal Society of London, series B.* 146:369–381.

Diederichs, K., J. Diez, G. Greller, C. Muller, J. Breed, C. Schnell, C. Vonrhein, W. Boos, and W. Welte. 2000. Crystal structure of MalK, the ATPase subunit of the trehalose/maltose ABC transporter of the archaeon Thermococcus litoralis. *EMBO J.* 19: 5951–5961.

Dousmanis, A.G., A.C. Nairn, and D.C. Gadsby. 2002. Distinct Mg(2+)-dependent steps rate limit opening and closing of a single CFTR Cl(-) channel. *J. Gen. Physiol.* 119:545–559.

Fersht, A. 1999. Structure and Mechanism in Protein Science. W. H. Freeman and Company, New York, NY. 631 pp.

Gadsby, D.C., and A.C. Nairn. 1994. Regulation of CFTR channel gating. *Trends Biochem. Sci.* 19:513–518.

Gadsby, D.C., and A.C. Nairn. 1999. Control of CFTR channel gating by phosphorylation and nucleotide hydrolysis. *Physiol. Rev.* 79:S77–S107.

Gao, M., H.R. Cui, D.W. Loe, C.E. Grant, K.C. Almquist, S.P. Cole, and R.G. Deeley. 2000. Comparison of the functional characteristics of the nucleotide binding domains of multidrug resistance protein 1. *J. Biol. Chem.* 275:13098–13108.

Gaudet, R., and D.C. Wiley. 2001. Structure of the ABC ATPase domain of human TAP1, the transporter associated with antigen processing. *EMBO J.* 20:4964–4972.

Guex, N., and M.C. Peitsch. 1997. SWISS-MODEL and the Swiss-PdbViewer: an environment for comparative protein modeling. *Electrophoresis.* 18:2714–2723.

Gunderson, K.L., and R.R. Kopito. 1994. Effects of pyrophosphate and nucleotide analogs suggest a role for ATP hydrolysis in cystic fibrosis transmembrane regulator channel gating. *J. Biol. Chem.* 269:19349–19353.

Gunderson, K.L., and R.R. Kopito. 1995. Conformational states of CFTR associated with channel gating: the role ATP binding and hydrolysis. *Cell.* 82:231–239.

Hopfner, K.P., A. Karcher, D.S. Shin, L. Craig, L.M. Arthur, J.P. Carney, and J.A. Tainer. 2000. Structural biology of Rad50 ATPase: ATP-driven conformational control in DNA double-strand break repair and the ABC-ATPase superfamily. *Cell.* 101:789–800.

Hou, Y., L. Cui, J.R. Riordan, and X.B. Chang. 2000. Allosteric interactions between the two non-equivalent nucleotide binding domains of multidrug resistance protein MRP1. *J. Biol. Chem.* 275:20280–20287.

Hou, Y.X., L. Cui, J.R. Riordan, and X.B. Chang. 2002. ATP binding to the first nucleotide-binding domain of multidrug resistance protein MRP1 increases binding and hydrolysis of ATP and trapping of ADP at the second domain. *J. Biol. Chem.* 277:5110–5119.

Hrycyna, C.A., M. Ramachandra, U.A. Germann, P.W. Cheng, I. Pastan, and M.M. Gottesman. 1999. Both ATP sites of human P-glycoprotein are essential but not symmetric. *Biochemistry.* 38: 13887–13899.

Hung, L.W., I.X. Wang, K. Nikaido, P.Q. Liu, G.F. Ames, and S.H. Kim. 1998. Crystal structure of the ATP-binding subunit of an ABC transporter. *Nature.* 396:703–707.

Hunke, S., M. Mourez, M. Jehanno, E. Dassa, and E. Schneider. 2000. ATP modulates subunit-subunit interactions in an ATP-binding cassette transporter (MalFGK2) determined by site-directed chemical cross-linking. *J. Biol. Chem.* 275:15526–15534.

Hwang, T.C., G. Nagel, A.C. Nairn, and D.C. Gadsby. 1994. Regulation of the gating of cystic fibrosis transmembrane conductance regulator Cl channels by phosphorylation and ATP hydrolysis. *Proc. Natl. Acad. Sci. USA.* 91:4698–4702.

Ikuma, M., and M.J. Welsh. 2000. Regulation of CFTR Cl^- channel gating by ATP binding and hydrolysis. *Proc. Natl. Acad. Sci. USA.* 97:8675–8680.

Jackson, M.B., B.S. Wong, C.E. Morris, H. Lecar, and C.N. Christian. 1983. Successive openings of the same acetylcholine receptor channel are correlated in open time. *Biophys. J.* 42:109–114.

Jones, P.M., and A.M. George. 1999. Subunit interactions in ABC transporters: towards a functional architecture. *FEMS Microbiol. Lett.* 179:187–202.

Junop, M.S., G. Obmolova, K. Rausch, P. Hsieh, and W. Yang. 2001. Composite active site of an ABC ATPase: MutS uses ATP to verify mismatch recognition and authorize DNA repair. *Mol. Cell.* 7:1–12.

Kaczmarek, L.K., K.R. Jennings, F. Strumwasser, A.C. Nairn, U. Walter, F.D. Wilson, and P. Greengard. 1980. Microinjection of catalytic subunit of cyclic AMP-dependent protein kinase enhances calcium action potentials of bag cell neurons in cell culture. *Proc. Natl. Acad. Sci. USA.* 77:7487–7491.

Karpowich, N., O. Martsinkevich, L. Millen, Y.R. Yuan, P.L. Dai, K. MacVey, P.J. Thomas, and J.F. Hunt. 2001. Crystal structures of the MJ1267 ATP binding cassette reveal an induced-fit effect at the ATPase active site of an ABC transporter. *Structure (Camb.).* 9:571–586.

Koronakis, E., C. Hughes, I. Milisav, and V. Koronakis. 1995. Protein exporter function and in vitro ATPase activity are correlated in ABC-domain mutants of HlyB. *Mol. Microbiol.* 16:87–96.

Li, C., M. Ramjeesingh, W. Wang, E. Garami, M. Hewryk, D. Lee, J.M. Rommens, K. Galley, and C.E. Bear. 1996. ATPase activity of the cystic fibrosis transmembrane conductance regulator. *J. Biol. Chem.* 271:28463–28468.

Linsdell, P., and J.W. Hanrahan. 1998. Adenosine triphosphate-dependent asymmetry of anion permeation in the cystic fibrosis transmembrane conductance regulator chloride channel. *J. Gen. Physiol.* 111:601–614.

Locher, K.P., A.T. Lee, and D.C. Rees. 2002. The *E. coli* BtuCD structure: a framework for ABC transporter architecture and mechanism. *Science.* 296:1091–1098.

Loo, T.W., and D.M. Clarke. 2001. Cross-linking of human multidrug resistance p-glycoprotein by the substrate, tris-(2-maleimidoethyl)amine, is altered by atp hydrolysis. evidence for rotation of a transmembrane helix. *J. Biol. Chem.* 276:31800–31805.

Manavalan, P., D.G. Dearborn, J.M. McPherson, and A.E. Smith. 1995. Sequence homologies between nucleotide binding regions

Published December 16, 2002

of CFTR and G-proteins suggest structural and functional similarities. *FEBS Lett.* 366:87–91.

Mathews, C.J., J.A. Tabcharani, and J.W. Hanrahan. 1998. The CFTR chloride channel: nucleotide interactions and temperature-dependent gating. *J. Membr. Biol.* 163:55–66.

Matsuo, M., N. Kioka, T. Amachi, and K. Ueda. 1999. ATP binding properties of the nucleotide-binding folds of SUR1. *J. Biol. Chem.* 274:37479–37482.

Matsuo, M., K. Tanabe, N. Kioka, T. Amachi, and K. Ueda. 2000. Different binding properties and affinities for ATP and ADP among sulfonylurea receptor subtypes, SUR1, SUR2A, and SUR2B. *J. Biol. Chem.* 275:28757–28763.

Moody, J.E., L. Millen, D. Binns, J.F. Hunt, and P.J. Thomas. 2002. Cooperative, ATP-dependent association of the nucleotide binding cassettes during the catalytic cycle of ATP-binding cassette transporters. *J. Biol. Chem.* 277:21111–21114.

Picciotto, M.R., J.A. Cohn, G. Bertuzzi, P. Greengard, and A.C. Nairn. 1992. Phosphorylation of the cystic fibrosis transmembrane conductance regulator. *J. Biol. Chem.* 267:12742–12752.

Powe, A.C.J., L. Al-Nakkash, M. Li, and T.C. Hwang. 2002. Mutation of Walker-A lysine 464 in cystic fibrosis transmembrane conductance regulator reveals functional interaction between its nucleotide-binding domains. *J. Physiol.* 539:333–346.

Qu, Q., and F.J. Sharom. 2001. FRET analysis indicates that the two ATPase active sites of the P-glycoprotein multidrug transporter are closely associated. *Biochemistry.* 40:1413–1422.

Quinton, P.M., and M.M. Reddy. 1992. Control of CFTR chloride conductance by ATP levels through non-hydrolytic binding. *Nature.* 360:79–81.

Ramjeesingh, M., C. Li, E. Garami, L.J. Huan, K. Galley, Y. Wang, and C.E. Bear. 1999. Walker mutations reveal loose relationship between catalytic and channel-gating activities of purified CFTR (cystic fibrosis transmembrane conductance regulator). *Biochemistry.* 38:1463–1468.

Riordan, J.R., J.M. Rommens, B. Kerem, N. Alon, R. Rozmahel, Z. Grzelczak, J. Zielenski, S. Lok, N. Plavsic, and J.L. Chou. 1989. Identification of the cystic fibrosis gene: cloning and characterization of complementary DNA. *Science.* 245:1066–1073.

Schneider, E., and S. Hunke. 1998. ATP-binding-cassette (ABC) transport systems: functional and structural aspects of the ATP-hydrolyzing subunits/domains. *FEMS Microbiol. Rev.* 22:1–20.

Schultz, B.D., C.J. Venglarik, R.J. Bridges, and R.A. Frizzell. 1995. Regulation of CFTR Cl^- channel gating by ADP and ATP analogues. *J. Gen. Physiol.* 105:329–361.

Senior, A.E., and S. Bhagat. 1998. P-glycoprotein shows strong catalytic cooperativity between the two nucleotide sites. *Biochemistry.* 37:831–836.

Sheppard, D.N., and M.J. Welsh. 1999. Structure and function of the CFTR chloride channel. *Physiol. Rev.* 79:S23–S45.

Szabó, K., G. Szakács, T. Hegeds, and B. Sarkadi. 1999. Nucleotide occlusion in the human cystic fibrosis transmembrane conductance regulator. Different patterns in the two nucleotide binding domains. *J. Biol. Chem.* 274:12209–12212.

Tabcharani, J.A., X.B. Chang, J.R. Riordan, and J.W. Hanrahan. 1991. Phosphorylation-regulated Cl^- channel in CHO cells stably expressing the cystic fibrosis gene. *Nature.* 352:628–631.

Ueda, K., N. Inagaki, and S. Seino. 1997. MgADP antagonism to Mg2+-independent ATP binding of the sulfonylurea receptor SUR1. *J. Biol. Chem.* 272:22983–22986.

Ueda, K., J. Komine, M. Matsuo, S. Seino, and T. Amachi. 1999. Cooperative binding of ATP and MgADP in the sulfonylurea receptor is modulated by glibenclamide. *Proc. Natl. Acad. Sci. USA.* 96: 1268–1272.

Urbatsch, I.L., L. Beaudet, I. Carrier, and P. Gros. 1998. Mutations in either nucleotide-binding site of P-glycoprotein (Mdr3) prevent vanadate trapping of nucleotide at both sites. *Biochemistry.* 37:4592–4602.

Urbatsch, I.L., B. Sankaran, J. Weber, and A.E. Senior. 1995. P-glycoprotein is stably inhibited by vanadate-induced trapping of nucleotide at a single catalytic site. *J. Biol. Chem.* 270:19383–19390.

Venglarik, C.J., B.D. Schultz, R.A. Frizzell, and R.J. Bridges. 1994. ATP alters current fluctuations of cystic fibrosis transmembrane conductance regulator: evidence for a three-state activation mechanism. *J. Gen. Physiol.* 104:123–146.

Vergani, P., C. Basso, A.C. Nairn, and D.C. Gadsby. 2002. Effects on CFTR Cl^- channel gating of Walker A lysine mutation K464A imply allosteric interaction between NBDs. *Biophys. J.* 82:240a.

Walker, J.E., M. Saraste, M.J. Runswick, and N.J. Gay. 1982. Distantly related sequences in the alpha- and beta-subunits of ATP synthase, myosin, kinases and other ATP-requiring enzymes and a common nucleotide binding fold. *EMBO J.* 1:945–951.

Weber, J., S.T. Hammond, S. Wilke-Mounts, and A.E. Senior. 1998. Mg2+ coordination in catalytic sites of F1-ATPase. *Biochemistry.* 37:608–614.

Weinreich, F., J.R. Riordan, and G. Nagel. 1999. Dual effects of ADP and adenylylimidodiphosphate on CFTR channel kinetics show binding to two different nucleotide binding sites. *J. Gen. Physiol.* 114:55–70.

Winter, M.C., D.N. Sheppard, M.R. Carson, and M.J. Welsh. 1994. Effect of ATP concentration on CFTR Cl^- channels: a kinetic analysis of channel regulation. *Biophys. J.* 66:1398–1403.

Yount, R.G. 1971. Adenylyl imidodiphosphate, an adenosine triphosphate analog containing a P-N-P linkage. *Biochemistry.* 10: 2484–2489.

Yuan, Y.R., S. Blecker, O. Martsinkevich, L. Millen, P.J. Thomas, and J.F. Hunt. 2001. The crystal structure of the mj0796 atp-binding cassette. implications for the structural consequences of atp hydrolysis in the active site of an abc transporter. *J. Biol. Chem.* 276: 32313–32321.

Zeltwanger, S., F. Wang, G.T. Wang, K.D. Gillis, and T.C. Hwang. 1999. Gating of cystic fibrosis transmembrane conductance regulator chloride channels by adenosine triphosphate hydrolysis. Quantitative analysis of a cyclic gating scheme. *J. Gen. Physiol.* 113:541–554.